

Biodiesel production from cooking palm oil in the presence of  $\text{CaO}/\gamma\text{-Al}_2\text{O}_3$  catalyst  
using rotating packed-bed reactor



A Thesis Submitted in Partial Fulfillment of the Requirements  
for the Degree of Master of Engineering in Chemical Engineering

Department of Chemical Engineering

Faculty of Engineering

Chulalongkorn University

Academic Year 2019

Copyright of Chulalongkorn University

การผลิตไบโอดีเซลจากน้ำมันปาล์มปรุงอาหารโดยใช้ตัวเร่งปฏิกิริยาแคลเซียมออกไซด์บนแกมมา  
อะลูมินาด้วยเครื่องปฏิกรณ์แบบแพคเบดที่ใช้แรงหมุนเหวี่ยง



วิทยานิพนธ์นี้เป็นส่วนหนึ่งของการศึกษาตามหลักสูตรปริญญาวิศวกรรมศาสตรมหาบัณฑิต  
สาขาวิชาวิศวกรรมเคมี ภาควิชาวิศวกรรมเคมี  
คณะวิศวกรรมศาสตร์ จุฬาลงกรณ์มหาวิทยาลัย  
ปีการศึกษา 2562  
ลิขสิทธิ์ของจุฬาลงกรณ์มหาวิทยาลัย

Thesis Title	Biodiesel production from cooking palm oil in the presence of CaO/ $\gamma$ -Al <sub>2</sub> O <sub>3</sub> catalyst using rotating packed-bed reactor
By	Miss Patcharaporn Sukjarern
Field of Study	Chemical Engineering
Thesis Advisor	Professor SUTTICHAJ ASSABUMRUNGRAT, Ph.D.
Thesis Co Advisor	Weerinda Appamana, D.Eng.

---

Accepted by the Faculty of Engineering, Chulalongkorn University in Partial Fulfillment of the Requirement for the Master of Engineering

..... Dean of the Faculty of Engineering  
(Professor SUPOT TEACHAVORASINSKUN, D.Eng.)

#### THESIS COMMITTEE

..... Chairman  
(Associate Professor DEACHA CHATSIRIWECH, Ph.D.)

..... Thesis Advisor  
(Professor SUTTICHAJ ASSABUMRUNGRAT, Ph.D.)

..... Thesis Co-Advisor  
(Weerinda Appamana, D.Eng.)

..... Examiner  
(CHUTIMON SATIRAPIPATHKUL, D.Eng.)

..... External Examiner  
(Issara Choedkiatsukul, D.Eng.)

พัชราภรณ์ สุขเจริญ : การผลิตไบโอดีเซลจากน้ำมันปาล์มปรุงอาหารโดยใช้ตัวเร่งปฏิกิริยาแคลเซียมออกไซด์บนแกมมาอะลูมินาด้วยเครื่องปฏิกรณ์แบบแพคเบดที่ใช้แรงหมุนเหวี่ยง. ( Biodiesel production from cooking palm oil in the presence of  $\text{CaO}/\gamma\text{-Al}_2\text{O}_3$  catalyst using rotating packed-bed reactor) อ.ที่ปรึกษาหลัก : ศ.ดร.สุทธิชัย อัสสะบำรุงรัตน์, อ.ที่ปรึกษาร่วม : ดร.วิรินทร์ดา อัมมานะ

วิทยานิพนธ์นี้เสนอการผลิตไบโอดีเซลจากน้ำมันปาล์มปรุงอาหารโดยใช้เครื่องปฏิกรณ์แบบแพคเบดโดยใช้แรงหมุนเหวี่ยง (rotating pack bed reactor, RPB) โดยการทดลองแบ่งออกเป็น 3 ส่วน คือ 1) การศึกษาการเตรียมตัวเร่งปฏิกิริยาวิวิธพันธ์  $\text{CaO}/\gamma\text{-Al}_2\text{O}_3$  และทดสอบความว่องไวต่อปฏิกิริยาทรานส์เอสเทอร์ฟิเคชันเครื่องปฏิกรณ์แบบกวนเชิงกลทั่วไป 2) การศึกษาการใช้ตัวเร่งปฏิกิริยา  $\text{CaO}/\gamma\text{-Al}_2\text{O}_3$  ในเครื่องปฏิกรณ์แบบ RPB และ 3) การศึกษาโดยใช้ตัวเร่งปฏิกิริยาโซเดียมไฮดรอกไซด์ ( $\text{NaOH}$ ) ในเครื่องปฏิกรณ์แบบ RPB ที่มีการบรรจุเบดที่เป็นวัสดุเฉื่อย โดยประยุกต์ใช้วิธีการพื้นผิวการตอบสนอง (RSM) บนพื้นฐานการออกแบบประสมกลาง (CCD) เพื่อลดจำนวนการทดลองให้น้อยลง ผลการทดลองพบว่า ภาวะที่เหมาะสมในการเตรียมตัวเร่งปฏิกิริยาคือ อุณหภูมิที่ใช้ในการแคลไซด์ เท่ากับ 500 องศาเซลเซียส ปริมาณแคลเซียมออกไซด์บนตัวรองรับแกมมาอะลูมินาเท่ากับ 24 เปอร์เซ็นต์โดยน้ำหนัก และให้ผลได้เมทิลเอสเทอร์เท่ากับ 88.56 เปอร์เซ็นต์ (%) ที่เวลา 1.5 ชั่วโมง ด้วยตัวเร่งปฏิกิริยา 3 เปอร์เซ็นต์โดยน้ำหนักของแคลเซียมออกไซด์เทียบกับน้ำมัน ซึ่งตัวเร่งปฏิกิริยาสามารถใช้ซ้ำได้ถึง 4 ครั้ง การใช้ตัวเร่งปฏิกิริยา  $\text{CaO}/\gamma\text{-Al}_2\text{O}_3$  ในเครื่องปฏิกรณ์แบบ RPB ให้ค่าร้อยละผลได้เมทิลเอสเทอร์ต่ำ นอกจากนี้การแพคเบดที่เป็นวัสดุเฉื่อยในเครื่องปฏิกรณ์แบบ RPB ช่วยเพิ่มผลได้เมทิลเอสเทอร์จาก 72.41 เป็น 86.20% เมื่อเทียบกับแบบไม่มีการแพคเบดที่เป็นวัสดุเฉื่อย ซึ่งภาวะที่เหมาะสมคือ อัตราส่วนโดยโมลระหว่างเมทานอลต่อน้ำมันเป็น 5.68:1 ปริมาณตัวเร่งปฏิกิริยา  $\text{NaOH}$  เป็น 1.27%, อัตราการไหลรวมที่ 130 มิลลิลิตรต่อนาที และความเร็วรอบการหมุน 1500 รอบต่อนาที ที่อุณหภูมิ 60 องศาเซลเซียส ให้ค่าผลได้เมทิลเอสเทอร์ 98.77% นอกจากนี้พบว่าผลได้ประสิทธิภาพ (yield efficiency) ในการผลิตไบโอดีเซลในเครื่องปฏิกรณ์แบบ RPB มีค่าสูงกว่าการใช้เครื่องปฏิกรณ์แบบกวนเชิงกลถึง 25 เท่า

สาขาวิชา วิศวกรรมเคมี

ลายมือชื่อนิสิต .....

ปีการศึกษา 2562

ลายมือชื่อ อ.ที่ปรึกษาหลัก .....

ลายมือชื่อ อ.ที่ปรึกษาร่วม .....

# # 6070256521 : MAJOR CHEMICAL ENGINEERING

KEYWORD: Rotating packed bed reactor (RPB); Biodiesel; heterogeneous catalyst; homogeneous catalyst; inert packing bed

Patcharaporn Sukjarern : Biodiesel production from cooking palm oil in the presence of  $\text{CaO}/\gamma\text{-Al}_2\text{O}_3$  catalyst using rotating packed-bed reactor. Advisor: Prof. SUTTICHA ASSABUMRUNGRAT, Ph.D. Co-advisor: Weerinda Appamana, D.Eng.

This thesis proposed the biodiesel production from cooking palm oil by using rotating pack bed reactor (RPB). The experiments were divided into 3 parts i) preparation of  $\text{CaO}/\gamma\text{-Al}_2\text{O}_3$  catalyst and catalytic activity for the transesterification in a conventional mechanical stirrer reactor (MS). ii) study of  $\text{CaO}/\gamma\text{-Al}_2\text{O}_3$  heterogeneous catalysts using RPB iii) study of NaOH homogeneous catalysts using RPB by packing inert packing bed. The Response surface methodology (RSM) based on the Central composite design (CCD) was used to reduce the number of experiments. The optimum condition for  $\text{CaO}/\gamma\text{-Al}_2\text{O}_3$  catalyst preparation was at calcination temperature of  $500^\circ\text{C}$  and  $24\%\text{CaO}/\gamma\text{-Al}_2\text{O}_3$ . 88.56% Fatty acid methyl ester (FAME yield) was obtained at 1.5 h in MS reactor. Moreover, the catalyst can be used repeatedly up to 4th cycle. The used of  $\text{CaO}/\gamma\text{-Al}_2\text{O}_3$  in RPB provided a low FAME yield. In addition, inert packing bed in RPB plays an important role in increasing FAME yield obtained from 72.41 to 86.20% compared to without using inert bed packing in RPB. The highest FAME yields as high as 98.77% was obtained at a methanol-oil molar ratio of 5.68:1, catalyst loading of 1.27%, total flow rate of 130 ml/min and rotational speed of 1500 rpm at  $60^\circ\text{C}$ . In addition, the yield efficiency of biodiesel production in RPB is 25 times higher than that of the MS.

Field of Study: Chemical Engineering

Academic Year: 2019

Student's Signature .....

Advisor's Signature .....

Co-advisor's Signature .....

## ACKNOWLEDGEMENTS

This research was supported by the TRF-CHE Research Grant for New Scholar (MRG 5980141) under the Thailand Research Fund and Office of the Higher Education Commission and the “Research Chair Grant” National Science and Technology Development Agency (NSTDA).

I would like to express appreciation to my advisor, Professor Dr. Suttichai Assabumrungrat, for sharing skill and valuable advice and encouragement extended to me. In addition, I wish to express my sincere thanks to Dr. Weerinda Appamana, my co-advisor, for her kind suggestions throughout my thesis and very patiently corrected my writing. I would grateful to thank to Associate Professor Deacha chatsiriwech as the chairman, Dr. Chitimon satirapipathkul as the examiner and Dr. Issara Choedkiatsakul as the external axaminer for good advice on my thesis.

In addition, I would like to thank all the teachers in the biodiesel group for the suggestion and help solve my problems. I appreciate scientist in Center of Excellence in Catalysis and Catalytic Reaction Engineering, Chulalongkorn University for chemical analysis and Rajamangala University of Technology Thanyaburi very much for chemical engineering laboratory throughout my study period.

Finally, I would like to thank to my family, they are part of my success. They always support me in every thing. Without them wouldn't have achieved this success. Thank you so much.

Patcharaporn Sukjarern

## TABLE OF CONTENTS

	Page
.....	iii
ABSTRACT (THAI) .....	iii
.....	iv
ABSTRACT (ENGLISH) .....	iv
ACKNOWLEDGEMENTS .....	v
TABLE OF CONTENTS .....	vi
LIST OF TABLES .....	xi
LIST OF FIGURES.....	xii
Chapter 1 Introduction .....	1
1.1 Introduction .....	1
1.2 Objective .....	3
1.3 Scope of works .....	3
1.4 Expected output.....	3
Chapter 2 .....	4
Theory.....	4
2.1 Cooking palm oil.....	4
2.2 Biodiesel .....	4
2.2.1 Reactions for biodiesel production .....	10
2.2.1.1 Transesterification .....	10
2.2.1.2 Esterification .....	11
2.2.2 Related reaction for biodiesel production.....	12

2.2.2.1 Hydrolysis.....	12
2.2.2.2 Saponification.....	13
2.3 Properties and standard of biodiesel.....	13
2.4 The Importance of a catalyst in the production of biodiesel.....	17
2.4.1 Base catalysts .....	17
2.4.1.1 Homogeneous base catalyst.....	17
2.4.1.2 Heterogeneous base catalyst.....	18
2.4.2 Acid catalysts.....	19
2.4.2.1 Homogeneous acid catalysts.....	20
2.4.2.2 Heterogeneous acid catalysts.....	20
2.5 Factors affecting biodiesel production.....	21
2.5.1 Temperature.....	21
2.5.2 Reaction time.....	21
2.5.3 Methanol to oil molar ratio.....	21
2.5.4 Type and amount of catalyst.....	22
2.5.5 Free fatty acid and water content.....	22
2.6 Spinning disk reactor (SDR).....	22
2.7 Design of experiment.....	23
2.7.1 Central Composite Designs .....	24
2.7.1.1 Determining $\alpha$ in Central Composite Designs .....	24
2.7.2 Box-Behnken designs .....	26
Chapter 3 Literature reviews.....	27
3.1 Conventional process for biodiesel production.....	27
3.2 Intensification reactors for biodiesel production.....	32



3.3 Spinning disc reactor for biodiesel production.....	36
3.4 Rotating reactor for biodiesel production.....	37
3.5 Mass transfer performance of rotating packed bed absorption.....	38
3.6 Response surface methodology.....	39
Chapter4 Experimental.....	41
4.1 Chemicals.....	41
4.2 Biodiesel production using heterogeneous catalyst.....	41
4.2.1 Catalyst preparation.....	41
4.2.2 Catalyst characterization.....	42
4.2.3 Experimental setup in conventional mechanical stirred reactor.....	42
4.2.4 Experimental setup in rotating packed reactor.....	43
4.3 Biodiesel production using homogeneous catalyst in RPB.....	45
4.3.1 Experimental set up.....	45
4.3.2 Design of experiments and optimization method.....	47
4.4 Analysis.....	48
4.5 Yield efficiency calculation.....	48
Chapter 5.....	49
Results and discussion.....	49
5.1 Biodiesel production in mechanical stirrer reactor using heterogeneous catalyst.....	49
5.1.1 Catalyst characterization.....	49
5.1.1.1 XRD studies.....	49
5.1.1.2 SEM-EDS analysis.....	50
5.1.2 Effect of calcination temperature on FAME yield.....	52

5.1.3 Effect of catalyst loading FAME yield .....	54
5.1.4 Effect of CaO loading on $\gamma$ -Al <sub>2</sub> O <sub>3</sub> .....	55
5.1.5 Evaluation of the catalyst reusability .....	55
5.2 Biodiesel production in rotating packed bed reactor using heterogeneous catalyst .....	56
5.3 Biodiesel production in rotating reactor using homogeneous catalyst .....	58
5.3.1 Effect of inert packing bed .....	58
5.3.2 CCD design.....	59
5.3.3 Response surface methodology .....	62
5.3.3.1 Effect of catalyst amount .....	62
5.3.3.2 Effect of methanol to oil molar ratio .....	64
5.3.3.3 Effect of rotational speed.....	66
5.3.3.4 Effect of flow rate.....	67
5.3.3.5 Response analysis of variance .....	68
5.3.3.6 Optimization of response parameters .....	70
5.4 Performance comparison of different reactors on biodiesel yield .....	71
Chapter 6 .....	74
Conclusions and recommendation .....	74
6.1 Conclusions.....	74
6.2 Recommendation.....	75
REFERENCES.....	76
Appendix A .....	87
Residence time calculation .....	87
Appendix B .....	88

Catalyst preparation .....	88
Appendix C .....	89
Yield efficiency calculation .....	89
VITA .....	90



## LIST OF TABLES

	Page
Table 1 Fatty Acid Composition of Typical Palm Oil and Its Components.....	6
Table 2 The properties of different vegetable oils [24]. .....	8
Table 3 Specifications of diesel and biodiesel fuels <sup>a</sup> [20]. .....	9
Table 4 U.S. and European specifications for biodiesel B100 and biodiesel blends [28]. .....	14
Table 5 Values of $\alpha$ as a function of the number of factors. ....	26
Table 6 Biodiesel production via different catalysts using conventional process.....	30
Table 7 Examples of biodiesel production processes via transesterification of oil using different variations of reactors.....	34
Table 8 The 3-factors, 5-levels CCD optimizing the operating condition of transesterification.....	40
Table 9 Independent variables used for CCD in transesterification.....	60
Table 10 Experimental design conditions and experimental results of the responses. .....	60
Table 11 Analysis of variance for response surface quadratic model.....	69
Table 12 Optimization for maximum biodiesel yield. ....	71
Table 13 Comparison performance of RPB with other reactors with different mixing types (catalyst loading = 1%wt of oil and reaction temperature = 60 °C). .....	73

## LIST OF FIGURES

	Page
Figure 1 Scheme for biodiesel production. ....	7
Figure 2 Transesterification of triglycerides with alcohol [24].....	10
Figure 3 Esterification of carboxylic with alcohol [25]. ....	11
Figure 4 Chemical reactions of hydrolysis to produce FFAs and water [26]. ....	12
Figure 5 Saponification process [27]. ....	13
Figure 6 Reaction mechanism of base-catalyzed transesterification [32]. ....	18
Figure 7 Reaction mechanism of acid-catalyzed transesterification [29] ....	19
Figure 8 The main structure of an SDR [40]. ....	23
Figure 9 Three types of central composite designs for two factors. ....	25
Figure 10 Three factors of Box-Behnken design. ....	26
Figure 11 RPB with blade packings. ....	39
Figure 12 Setup of conventional mechanical stirred reactor.....	43
Figure 13 Set up of the RPB-MS reactor. ....	44
Figure 14 Schematic of experimental RPB apparatus used for heterogeneously catalyzed transesterification reaction. ....	45
Figure 15 Schematic of experimental RPB apparatus used for homogeneous catalyzed transesterification reaction. ....	46
Figure 16 Setup of the RPB reactor. ....	47
Figure 17 XRD patterns for samples (a) $\gamma$ -Al <sub>2</sub> O <sub>3</sub> , catalysts obtained from the nitrate precursor; (b) 400 °C, (c) 500 °C, (d) 600°C, (e) 700°C; ■, ●, ▲, ◆ : $\gamma$ -Al <sub>2</sub> O <sub>3</sub> , CaO, Ca(OH) <sub>2</sub> and Ca(NO <sub>3</sub> ) <sub>2</sub> , respectively. ....	50

Figure 18 SEM images of the catalyst carrier, support ( $\gamma$ -Al <sub>2</sub> O <sub>3</sub> ) (a), catalyst derived from the nitrate precursor calcined at 400 °C (b), 500 °C (c), 600°C (d) and 700 °C (e), respectively and EDS for 500 °C (f).....	51
Figure 19 EDS images of the CaO/ $\gamma$ -Al <sub>2</sub> O <sub>3</sub> catalyst at 500 °C.....	52
Figure 20 The effect of calcination temperature on FAME yielded.....	53
Figure 21 Effect of catalyst loading on FAME yield. (molar ratios of 12, 0.5 - 3 %wt CaO to the oil and temperature of 60 °C).....	54
Figure 22 Effect of CaO loading on $\gamma$ -Al <sub>2</sub> O <sub>3</sub> (molar ratios of 12, 8 - 24 %CaO/ $\gamma$ -Al <sub>2</sub> O <sub>3</sub> and temperature of 60 °C).....	55
Figure 23 The reusability of the CaO/ $\gamma$ -Al <sub>2</sub> O <sub>3</sub> catalyst without pretreatment in batch process. ....	56
Figure 24 Effect of reaction time for RPB reactor on biodiesel yield. ....	57
Figure 25 Comparison of cases with inert packing bed of hollow cylinder and without inert bed packing on the transesterification. ....	59
Figure 26 3D Plot of the interaction effects of (a) catalyst amount and molar ratio, (b) catalyst amount and rotational speed, (c) catalyst amount and flow rate on the transesterification.....	63
Figure 27 3D Plot of the interaction effects of (a) molar ratio and rotational speed, (b) molar ratio and flow rate on the transesterification.....	65
Figure 28 Comparison of the experimental and predicted values of biodiesel yield..	70
Figure 29 Optimized results of response. ....	71

## Chapter 1

### Introduction

#### 1.1 Introduction

Nowadays, the energy demand continuously increases because of the lack of fossil fuels such as oil and petroleum, causing the requirement of renewable and sustainable fuels. Biodiesel has lately become a promising replacement for petroleum diesel fuel because its high heating value is nearly equivalent to diesel fuels, and it presents low environmental impact. Biodiesel is commonly produced by chemical transesterification which transforms triglyceride and methanol into fatty acid methyl esters (FAMES). The most commonly prepared esters are methyl esters because methanol is the least expensive alcohol. In addition, methanol has a small molecule than ethanol, so it reacts better than ethanol. The major feedstock used to produce biodiesel are such as vegetable oils and animal fats using homogeneous (acid and alkaline) or heterogeneous catalysts [1, 2].

Homogeneous catalysts such as sodium methoxide and potassium methoxide are usually used for biodiesel production since they have the advantage of providing high catalytic activity under mild conditions [3, 4]. Unfortunately, the process involving homogeneous catalysts has some limitations such as production of soap as a side product and large requirement of water for the separation and cleaning of catalyst, resulting higher production cost [5, 6]. In contrast, heterogeneous catalysts are potentially low cost and can solve many of the problems encountered in homogeneous catalysts. The loading of alkali and alkaline earth elements and oxides on alumina support followed by an activation treatment at high temperature has been applied to synthesize an efficient solid-phase catalyst for the transesterification of triacylglycerols even though alumina itself exhibits activity [1, 7, 8]. Lately, an increasing number of researchers has examined systems consisted of CaO loaded on a carrier. Among metals oxide loaded on  $\text{Al}_2\text{O}_3$ ,  $\text{CaO}/\gamma\text{-Al}_2\text{O}_3$  catalysts proved to be more active than oxides of other metals [1]. However, there is a big hurdle in the process with heterogeneous catalysts. The reaction rate is slow due to diffusion problems between the three phases (oil/methanol/solid media) in the presence of a heterogeneous

catalyst [1]. This is the reason that many research groups pointed out transesterification being a mass transfer-controlled reaction, and the solid–liquid mass transfer resistance between reactants and solid catalyst is the cause for the extremely long reaction time, resulting in a low process efficiency [1, 9].

Therefore, increasing the efficiency of mass transfer can help increase rate of the reaction and yield efficiency. To resolve these problems, intensification processes can be employed. Rotating packed beds (RPB) have received considerable attention as a method of process intensification. RPBs have been designed to generate high centrifugal acceleration, providing a good dispersion for a two-phase flow. By having liquid flow through the porous packing in the rotor, it is split into micro droplet or nano-droplet and thin films, and there is also an excellent renewed two-phase interface [10]. In order to further enhance the performance of the RPB reactor, various rotors with different structures have been designed [11-13]. For example, a multi liquid-inlet rotating packed bed (MLI-RPB) reactor has 23% higher gas-liquid effective interfacial area, 8% higher gas-liquid mass-transfer coefficient, and 50% lower pressure drop than the traditional RPB reactor [14]. It can be seen that a reasonable design of packing bed is insignificant for liquid flow and mass transfer improvement.

The objective of this study is to develop a new technique for the biodiesel production using a RPB as the transesterification reactor. The methanolysis of cooking palm oil (CPO) with  $\text{CaO}/\gamma\text{-Al}_2\text{O}_3$  and NaOH catalysts is carried out in the RPB. The effect of inert packing bed was studied in RPB. For optimization of the operating parameters (catalyst loading, reactant ratio, rotational speed and feed flow rate) of the reaction, statistical approach as response surface methodology (RSM) was used as it reduced the number of experimental trials needed to evaluate multiple factors and their interactions [15]. Considering this analysis, central composite design (CCD) design with four operating parameters each having three factorial values was used in the present work. In addition, the reactor performance and energy efficiency were considered and compared to those of a conventional mechanical stirred reactor (MS).



## 1.2 Objective

To study the performance of rotating pack bed reactor including with and without inert bed packing for the biodiesel production from transesterification of cooking palm oil using homogeneous and heterogeneous catalysts.

## 1.3 Scope of works

1.3.1 The catalysts were prepared by wet impregnation method using calcium nitrate precursor loading between 8- 24% wt of CaO on  $\gamma$ -Al<sub>2</sub>O<sub>3</sub> and the catalysts calcination temperature was between 400-700 °C.

1.3.2 The catalytic activity CaO/ $\gamma$ -Al<sub>2</sub>O<sub>3</sub> was tested in transesterification of cooking palm oil using a mechanical stirred tank reactor (MS) and the catalyst reusability on the yield of biodiesel was investigated.

1.3.3 Improving biodiesel production rate by using rotating packed bed reactor (RPB). For the transesterification of cooking palm oil via CaO/  $\gamma$ - Al<sub>2</sub>O<sub>3</sub> catalyst was investigated.

1.3.4 The optimum conditions by using response surface methodology (RSM) based on central composite design (CCD) for transesterification of cooking palm oil via NaOH catalyst in RPB were determined. Various parameters which affect biodiesel production such as inert bed, molar ratio of methanol to oil, flow rate, rotational speed and catalyst amount were studied.

1.3.5 The biodiesel production performance of rotating packed bed reactor (RPB) and the mechanical stirrer reactor (MS) was compared based on their yield efficiency.

## 1.4 Expected output

To obtain the optimal condition and the maximum performance for producing biodiesel of rotating packed bed reactors for biodiesel production via transesterification of cooking palm oil.

## Chapter 2

### Theory

#### 2.1 Cooking palm oil

Biodiesel can be achieved from different feedstocks such as vegetable, microbial oil and animal fats. The selection of feedstock is influenced by various factors such as purity of biodiesel, cost, composition and yield. Type of feedstocks source are the main parameters for categorization of biodiesel such as edible and non-edible oil [16]. Selection of feedstocks is also reliant on regions. Availability and economic of country was considered before selecting feedstock such as cooking palm oil is used as feedstock in Thailand. Use of edible feedstock for the biodiesel production is popular at the beginning of the biodiesel era. The physical properties of palm oil include solid fat content, viscosity, density, specific gravity, and refractive index. Cooking palm oil differs from many common vegetable oils such as a high level of palmitic acid approximately 44%. In general, cooking palm oil consists of approximately 50% saturated fatty acids, 40% monounsaturated fatty acids, and 10% polyunsaturated fatty acids [17]. Table 1 shows the typical FA compositions of cooking palm oil and components by Tan & Che Man (2000) [18] in comparison with Firestone's report (2006) [19].

#### 2.2 Biodiesel

Biodiesel is one of the most perspective alternative fuels since it is a non-toxic and can be produced from different renewable sources. The advantages of biodiesel are that it displaces petroleum thereby reducing global warming gas emissions, hydrocarbons, carbon monoxide, and other air toxics [20]. Today, 95% of world biodiesel production is produced from edible oil feedstock, such as soybean oil, palm oil, castor seed oil and algal oil etc. [21, 22]. Table 2 shows the major triglycerides composition for different oil feedstock. The transesterification reaction is the most common method of biodiesel production, where triglycerides are converted into fatty acid esters using homogeneous (acid and alkaline) or heterogeneous catalysts.

Furthermore, the use of biodiesel is a lower pollution than that of diesel fuel. Selected properties of diesel and biodiesel fuels are given in Table 3. It is found that diesel

and biodiesel are similar properties. The advantages of biodiesel fuel is lower sulfur content than diesel oil. Biodiesel production process can be divided into 4 methods such as direct use and blending, micro emulsion process, thermal cracking process and transesterification process [23]. First method is direct use and blending, the direct use of vegetable oils with adding some chemical modification in diesel engine is problematic. Although some diesel engine can run pure vegetable oils, energy consumption with the use of pure vegetable oils was found to be homologous to the diesel fuel for short term use, ratio of 1:10 to 2:10 oil to diesel. Second method is micro-emulsion process, the trouble of the high viscosity of vegetable oils was corrected by micro-emulsions with solvents such as methanol, ethanol, and 1-butanol. Micro emulsion is defined as the colloidal equilibrium dispersion of optically isotropic fluid microstructures with dimensions normally in the range of 1–150 nm. The components of a biodiesel micro- emulsion include diesel fuel, vegetable oil, alcohol, and surfactant and cetane improver in appropriate proportions. Alcohols are used as viscosity lowering additives, higher alcohols are used as surfactants and alkyl nitrates are used as cetane adjusters. Micro-emulsion results in reduction in viscosity enhance in cetane number and good spray characters in the biodiesel. Third method is thermal cracking (pyrolysis), pyrolysis is called the conversion of one substance into another by means of heat. It involves heating in the absence of air or oxygen and breakage of chemical bonds to yield small molecules. The pyrolysis of vegetable oil to produce biofuels was found to produce alkanes, alkenes, alkadienes, aromatics and carboxylic acids in various proportions. Furthermore, the removal of oxygen during the thermal processing also removes any environmental benefits. Drawbacks of pyrolysis is the need for separate distillation wherewith the product obtained is similar gasoline containing sulphur which makes it less ecofriendly. Finally, transesterification and esterification method which, are the most common method to produce biodiesel [22]. Figure 1 shows as biodiesel production process via transesterification and esterification from fresh and waste cooking oil, respectively.

**Table 1** Fatty Acid Composition of Typical Palm Oil and Its Components.

Fatty acid (%)	PO		PO <sub>O</sub>		PO <sub>S</sub>		PKO	
	Results <sup>1</sup>	Range <sup>2</sup>	Results <sup>1</sup>	Range <sup>2</sup>	Results <sup>1</sup>	Range <sup>2</sup>	Results <sup>1</sup>	Range <sup>2</sup>
C6:0	-	-	-	-	-	-	0.5	0-0.8
C8:0	-	-	-	-	-	-	6.4	1.9-6.2
C10:0	-	-	-	-	-	-	5.2	2.6-5.0
C12:0	0.5	0-0.4	0.7	0.1-0.5	0.4	0.1-0.4	55.8	40-55
C14:0	1.7	0.5-2.0	1.5	0.9-1.4	2.1	1.1-1.8	14.7	14-18
C16:0	48.7	40-48	41.6	38.2-42.9	68.3	48.7-73.8	5.8	6.5-10.3
C16:1	-	0-0.6	-	0.1-0.3	-	0.05-0.2	-	-
C18:0	3.9	3.5-6.5	3.8	3.7-4.8	4.0	3.9-5.6	1.3	1.3-3
C18:1	37.1	36-44	42.0	39.8-43.9	20.6	15.6-36.0	8.9	12-21
C18:2	8.1	6.5-12.0	10.4	10.4-13.4	4.6	3.2-9.8	1.5	1-3.5
C18:3	-	0-0.5	-	0.1-0.6	-	0.1-0.6	-	0-0.7
C20:0	-	0-1	-	0.2-0.6	-	0.3-0.6	-	0-0.3
C20:1	-	0-0.2	-	--	-	-	-	0-0.5
C22:0	-	0-0.1	-	-	-	-	-	-
C24:0	-	0-0.2	-	-	-	-	-	-

Abbreviations: RBDPO, palm oil; PO<sub>O</sub>, palm olein; PO<sub>S</sub>, palm stearin; PKO, palm kernel oil.

1 Authors' own findings.

2 Source: Firestone

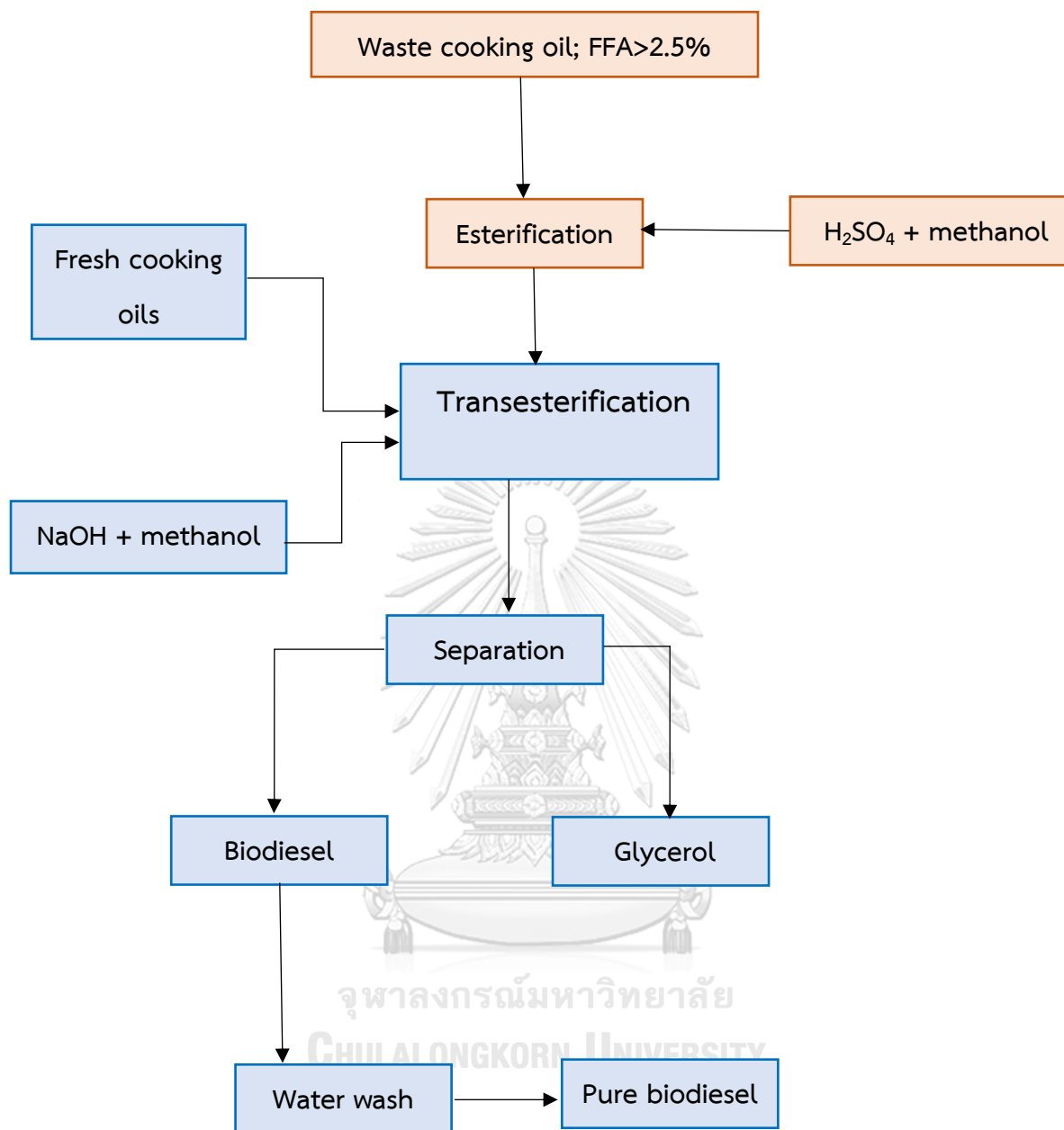


*Figure 1* Scheme for biodiesel production.

**Table 2** The properties of different vegetable oils [24].

Type of Oil	Species	Fatty acid composition (wt%)	Viscosity (at 40 °C)	Density (g/cm <sup>3</sup> )	Flash point (°C)	Heating value (MJ/kg)	Acid value (mg KOH/g)	Cetane number (C)	Cloud point (°C)	Pour point (°C)
Edible oil	Soybean	C16:0, C18:1, C18:2	32.9	0.91	254	39.6	0.2	37.9	-3.9	-12.2
	Rapeseed	C16:0, C18:0, C18:1, C18:2	35.1	0.91	246	39.7	2.92	37.6	3.9	-31.7
	Sunflower	C16:0, C18:0, C18:1, C18:2	32.6	0.92	274	39.6	-	41.3	18.3	-6.7
	Palm	C16:0, C18:0, C18:1, C18:2	39.6	0.92	267	-	0.1	42.0	31.0	-
	Peanut	C16:0, C18:0, C18:1, C18:2, C20:0, C22:0	22.72	0.90	271	39.8	3	41.8	12.8	-6.7
	Corn	C16:0, C18:0, C18:1, C18:2, C18:3	34.9	0.91	277	39.5	-	37.6	1.1	-40.0
	Camelina	C16:0, C18:0, C18:1, C18:2, C18:3, C20:0, C20:1, C20:3	-	0.91	-	42.2	0.76	-	-	-
	Canola	C16:0, C18:0, C18:1, C18:2, C18:3	38.2	-	-	-	0.4	-	-	-
	Cotton	C16:0, C18:0, C18:1, C18:2	18.2	0.91	234	39.5	-	41.8	1.7	-5.0
	Pumpkin	C16:0, C18:0, C18:1, C18:2	35.6	0.92	>230	39	0.55	-	-	-
Non-edible oil	Jatropha curcas	C16:0, C16:1, C18:0, C18:1, C18:2	29.4	0.92	225	38.5	28	-	-	-
	Pongamia pinnata oil	C16:0, C18:0, C18:1, C18:2, C18:3	27.8	0.91	205	34	5.06	-	-	-
	Sea mango	C16:0, C18:0, C18:1, C18:2	29.6	0.92	-	40.86	0.24	-	-	-
	Palanga	C16:0, C18:0, C18:1, C18:2	72.0	0.90	221	39.25	44	-	-	-
	Tallow	C14:0, C16:0, C16:1, C17:0, C18:0, C18:1, C18:2	-	0.92	-	40.05	-	-	-	-
Others	WCO	Depends on fresh cooking oil	44.7	0.90	-	-	2.5	-	-	-
-	Diesel	-	3.06	0.855	76	43.8	-	50	-	-16

**Table 3** Specifications of diesel and biodiesel fuels<sup>a</sup> [20].

Fuel property	Diesel	Biodiesel
Fuel standard	ASTM D975	ASTM PS 121
Fuel composition	C10 – C21 HC	C12-C22 FAME
Lower heating value (MJ/m <sup>3</sup> )	36.6 × 10 <sup>3</sup>	32.6 × 10 <sup>3</sup>
Kinematic viscosity @ 40 °C (mm <sup>2</sup> /s)	1.3 – 4.1	1.9 – 6.0
Specific gravity @ 15.5 °C	0.85	0.88
Density @ 15 °C (kg/m <sup>3</sup> )	848	878
Water (ppm by wt.)	161	0.05% max
Carbon (wt.%)	87	77
Hydrogen (wt.%)	13	12
Oxygen (by diff.) (wt.%)	0	11
Sulfur (wt.%)	0.05 max	0.0 – 0.0024
Boiling point (°C)	188-343	182–338
Flash point (°C)	60-80	100–170
Cloud point (°C)	-15 to 5	-3 to 12
Pour point (°C)	-35 to -15	-15 to 10
Cetane number	40 - 55	48 - 65
Stoichiometric air/fuel ratio (wt./wt.)	15	13.8

a

From: Tyson, KS *biodiesel handling and use guidelines* National Renewable Energy Laboratory NREL/TP-580-30004 September 2001.

## 2.2.1 Reactions for biodiesel production

### 2.2.1.1 Transesterification

Transesterification, also called alcoholysis, is a chemical reaction of an oil or fat with an alcohol in the presence of a catalyst to form esters and glycerol. It involves a sequence of three consecutive reversible reactions where triglycerides (TGs) are sequentially (eqs.1-3) converted to diglycerides, monoglycerides, and finally glycerol (by product). In each step an ester is produced and thus three ester molecules are produced from one molecule of TG. The short chain alcohols such as methanol, ethanol, and butanol are frequently used, with methanol being the most common. However, methanol is preferred because of its low cost. Figure 2 shows the transesterification reaction of TGs with alcohol. A catalyst is usually used to enhance the reaction rate and yield because the reaction is reversible and excess alcohol is used to shift the equilibrium to the product side [24].

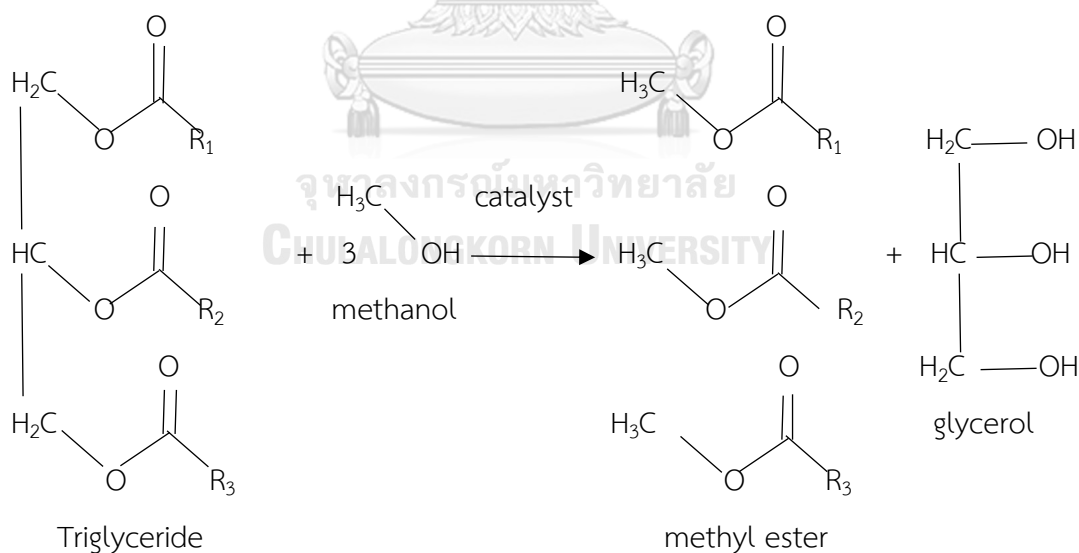
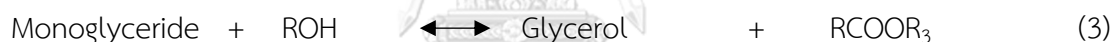


**Figure 2** Transesterification of triglycerides with alcohol [24].



### 2.2.1.2 Esterification

Esterification is a chemical reaction that occurs between the acid (usually carboxylic acid) and the alcohol where esters are achieved. The reaction occurs in acidic environments. In this process, water is also obtained. Its fall into the category of “condensation reactions” as shown in Figure 3.

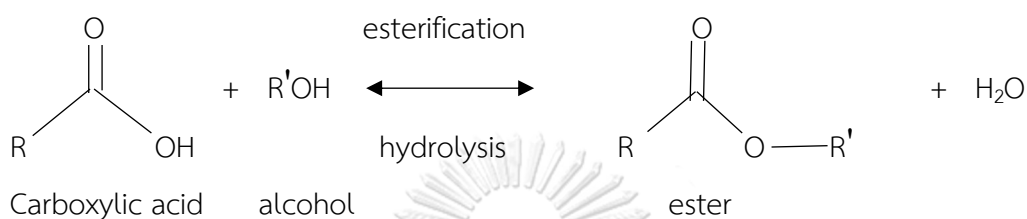


**Figure 3** Esterification of carboxylic with alcohol [25].

The reaction between carboxylic acid to alcohol is known as the Fischer esterification. When a carboxylic acid and an alcohol are mixed bring in no reaction takes place. However, upon addition of catalytic amounts of an acid, the two components together in an equilibrium process to give an ester and water. The acid catalyst in the mechanism of ester formation helps in two ways:

- Acid catalyst causes the carbonyl function (makes the carbonyl carbon more electrophilic) to undergo nucleophilic attack by the alcohol.
- Protonation of the hydroxyl group provide water, which is a superior leaving group (i.e. weaker base) in the elimination step.

The most common used catalysts for a Fischer esterification include sulfuric acid, p-toluene sulfonic acid (tosylic acid), and Lewis acids.

## 2.2.2 Related reaction for biodiesel production.

### 2.2.2.1 Hydrolysis

Reaction mechanism takes place in three steps. For the first step, the triglyceride is converted into diglyceride. Next, the diglyceride is converted into monoglyceride. Finally, the monoglyceride is converted into glycerol. Every stepwise generates a product known as FFAs as shown in Figure 4. The water to oil molar ratio is a significant parameter of hydrolysis reaction and stoichiometric ratio requires 3 moles of water and 1 mole of oil. An excess water will take the system equilibrium towards to final products (fatty acids and glycerol).

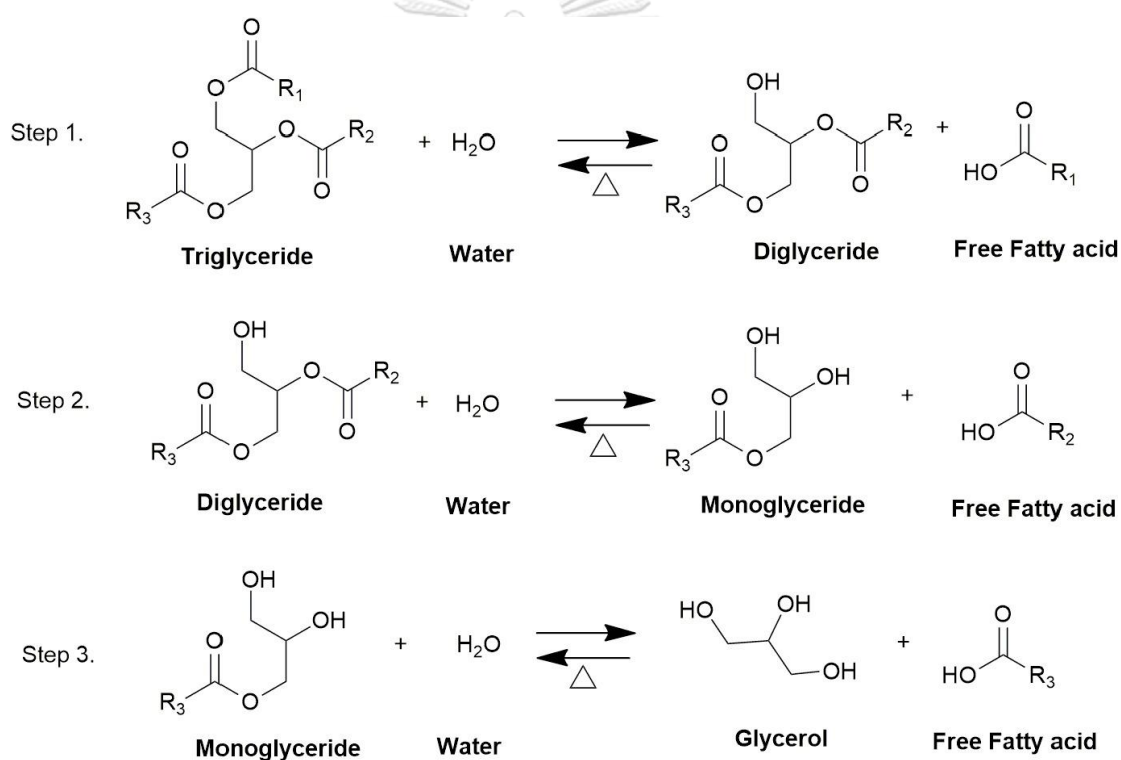


**Figure 4** Chemical reactions of hydrolysis to produce FFAs and water [26].

### 2.2.2.2 Saponification

When triglycerides in transesterification react with aqueous NaOH or KOH, they are shifted into soap and glycerol as shown in Figure 5. This is known as alkaline hydrolysis of esters because the reaction leads to the formation of soap, it is called the saponification process. The saponification reaction is exothermic which heat is liberated during the process.

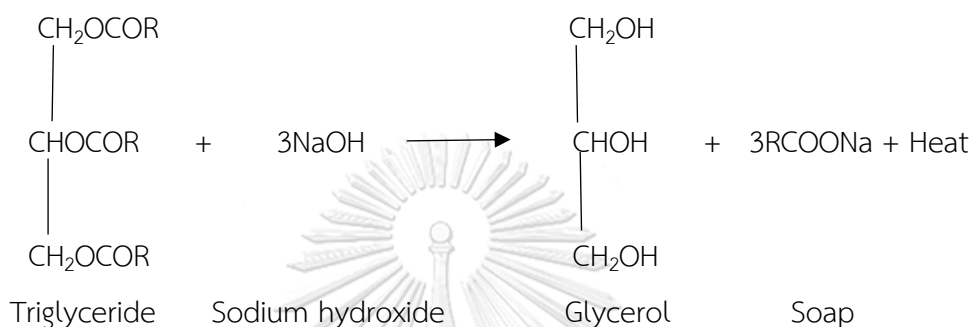


**Figure 5** Saponification process [27].

### 2.3 Properties and standard of biodiesel

When reviewing the properties of biodiesel, the standard specifications have been established by various fuel standard-setting organizations, particularly ASTM (in the U.S.) and the European Committee for Standardization (CEN). ASTM has established standard specifications for biodiesel fuel blend stocks (B100), known as ASTM D6751. Nowadays, the CEN has only established standard specifications for B100, known as EN 14214. Table 4 shows a side-by-side listing of specifications for biodiesel blend stock (B100; ASTM and CEN) and mid-level biodiesel blends (B6–B20; ASTM only) [28].

**Table 4** U.S. and European specifications for biodiesel B100 and biodiesel blends [28].

Property	Biodiesel (B100)				B6-B20 blends	
	U.S. (ASTM D6751-08)		Europe (EN 14214)		U.S. (ASTM D7467-08)	
	Limits	Method	Limits	Method	Limits	Method
Water and sediment (vol%, max)	0.05	D2709	0.05	EN12937	0.05	D2709
Total contamination (mg/kg, max)	-	-	24	EN12662	-	-
Kinematic viscosity @ 40°C (mm <sup>2</sup> /s)	1.9-6.0	D445	3.5-5.0	EN3104/ 3105	1.9-4.1	D445
Flash point, closed cup (°C, min)	93	D93	101	EN3679	52	D93
Methanol (wt.%, max)	0.20	EN14110	0.20	EN14110	-	-
Cetane no. (min)	47	D613	51	EN5165	40	D613
Cloud point (°C)	Report	D2500	Country Specific	-	Report	D2500
Sulfated ash (wt.%, max)	0.020	D874	0.020	EN3987	-	-
Total ash (wt.%, max)	-	-	-	-	0.01	D482
Gp I metals Na + K (mg/kg, max)	5.0	EN14538	5.0	EN14108 /14109	-	-
Gp II Metals Ca + Mg (mg/kg, max)	5.0	EN14538	5.0	EN14538	-	-

**Table 4** U.S. and European specifications for biodiesel B100 and biodiesel blends (cont.) [28].

Property	Biodiesel (B100)		B6-B20 blends			
	U.S. (ASTM D6751-08)		Europe (EN 14214)		U.S. (ASTM D7467-08)	
	Limits	Method	Limits	Method	Limits	Method
Total Sulfur (ppm, max)	15	D5453	10	EN20846	15	D5453
Phosphorous (ppm, max)	10	D4951	4	EN14107	-	-
Acid no. (mg KOH/g, max)	0.50	D664	0.50	EN14104	0.3	D664
Carbon residue (wt.%, max)	0.05	D4530	0.30	EN10370	0.35	D524
Free glycerin (wt.%, max)	0.02	D6584	0.02	EN14105 /14106	-	-
Total glycerin (wt.%, max)	0.24	D6584	0.25	EN14105	-	-
Mono glyceride (wt.%, max)	-	-	0.80	EN14105	-	-
Diglyceride (wt.%, max)	-	-	0.20	EN14105	-	-
Triglyceride (wt.%, max)	-	-	0.20	EN14105	-	-
Distillation (T90°C, max)	36	D1160	-	-	343	D86

**Table 4** U.S. and European specifications for biodiesel B100 and biodiesel blends (cont.) [28].

Property	Biodiesel (B100)		Europe (EN 14214)		B6-B20 blends	
	U.S. (ASTM D6751-08)		Europe (EN 14214)		U.S. (ASTM D7467-08)	
	Limits	Method	Limits	Method	Limits	Method
Copper strip corrosion (3-h at 50° C, max)	No.3	D130	No.1	EN2160	No.3	D130
Oxidation Stability (h @ 110°C, min)	3.0	EN14112	6.0	EN14112	6	EN14112
Linolenic acid methyl ester (wt.%, max)	-	-	12.0	EN14103	-	-
Polyunsaturated acid methyl esters (wt.%, max)	-	-	1.0	prEN15799	-	-
Ester Content (wt.%, min)	-	-	96.5	EN14103	6-20 vol.%	D7371
Iodine Value (g I <sub>2</sub> /100 g, max)	-	-	120	EN14111	-	-
Density (kg/m <sup>3</sup> )	-	-	860-900	EN3675	-	-
Lubricity @ 60°C, WSD, microns (max)	-	-	-	-	520	D6079
Cold Soak Filterability (seconds, max)	360	D7501	-	-	-	-

## 2.4 The Importance of a catalyst in the production of biodiesel

The catalysts for transesterification of biodiesel are broadly divided into two types include base catalysts and acid catalysts. Base catalysts are desired over acid catalysts. The researchers studied the base catalysts successfully when the free fatty acid (FFA) is less than one percentage, but it was also observed can be used in cases where the FFA content is greater than one. After that, base catalyst exhibit excellent result when the FFA content of the oil is below two. It has also been shown that the rate of the reaction becomes a thousand times faster when a base catalyst is used instead of an acid catalyst.

### 2.4.1 Base catalysts

The three steps of the reaction mechanism is shown in Figure 6. The first step is the reaction carbonyl carbon atom with the anion of the alcohol. After that, forming a tetrahedral intermediate. Finally step, from which the alkyl ester and corresponding anion of the DG [29].

#### 2.4.1.1 Homogeneous base catalyst

Homogeneous base catalysts have been widely used for biodiesel due to their rather high catalytic activity and higher biodiesel conversion under mild conditions [3]. Base catalyst is reaction faster than acids [30]. The most common catalyst are sodium hydroxide, sodium methoxide, potassium hydroxide and potassium methoxide which, its very efficient in achieving high conversion rates [31]. However, the disadvantage of base catalyzed process is saponification as a side reaction, the formation of undesirable amounts of soap and large quantities of wastewater impacting the environment for separation process produces [23]. Figure 6 shows as the reaction mechanism of base-catalyzed transesterification for biodiesel production.

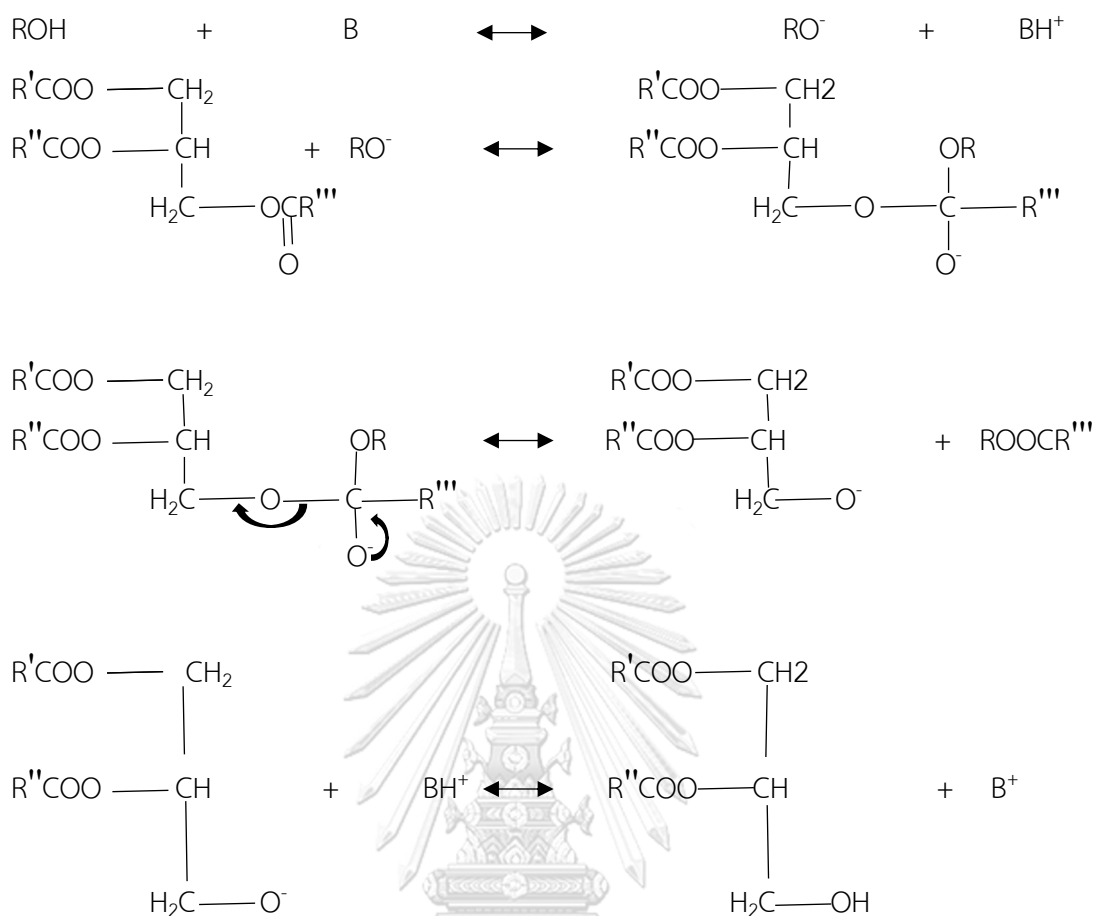


**Figure 6** Reaction mechanism of base-catalyzed transesterification [32].

#### 2.4.1.2 Heterogeneous base catalyst

The main mechanism of heterogeneous catalysis follows the principle similar to homogeneous catalysis. The catalyst efficiency depends on specific surface area, pore size, pore volume and active site concentration. The order of activity among alkaline earth oxide catalysts include  $\text{BaO} > \text{SrO} > \text{CaO} > \text{MgO}$  [33]. Alkaline earth metal compounds are heterogeneous catalysts and dispersion in the reaction has a massive effect on the level of their catalytic activity determined by diffusion. The structure of metal oxides is consist of positive metal ions (cations) whereof possess Lewis acidity. It serves as electron acceptors, and negative oxygen ions (anions) which serve as proton acceptors and are thus Brønsted bases. The most common solid base catalysts are alkaline earth metal oxides, zeolites,  $\text{KNO}_3/\text{Al}_2\text{O}_3$ ,  $\text{BaO}$ ,  $\text{SrO}$ ,  $\text{CaO}$  and  $\text{MgO}$ .



Consequently, heterogeneous base catalysts are insoluble, separated simply by filtration and can be reused [23].

#### 2.4.2 Acid catalysts

Although base catalyst is popular for transesterification. These do not exhibit good results when feedstock contains water and high acid value. Base catalysts are highly sensitive to water which will result in soap formation, separation difficult. The mechanism of the acid catalyzed transesterification is shown in Figure 7. Transesterification process by acids gives high FAME and not soap formation during the process, but the reactions are slow. However, acid catalyst required long time to react and higher catalyst amounts, which is more expensive than basic catalysts. The conversion of triglycerides to biodiesel using an acid catalyst is also known as esterification.

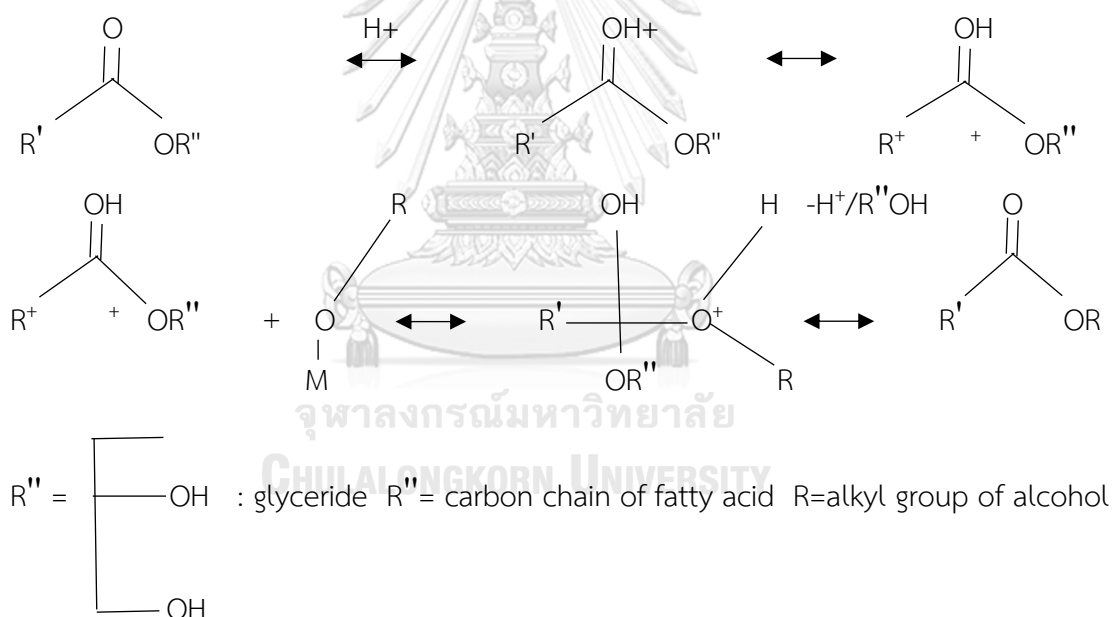


**Figure 7** Reaction mechanism of acid-catalyzed transesterification [29]

#### 2.4.2.1 Homogeneous acid catalysts.

Homogeneous acid catalysts such as sulfuric acid ( $H_2SO_4$ ) and hydrochloric acid (HCl) are preferred for feedstock that contains high FFA. They are most widely used due to strong acidic properties and low cost. However, it is reported that  $H_2SO_4$  shows better performance on biodiesel yield than HCl in transesterification [34]. In addition, the advantages of using acidic catalysts are insensitive to FFA content in the oil and avoidance of side reaction [35]. In addition, acidic catalysts can produce esterification and transesterification at the same time. Esterification reaction occurs when FFA reacts with alcohol in the presence of acidic catalysts to create esters as reaction products. This is the most commonly used method for reducing FFA. However, homogeneous acid catalysts posed many disadvantages, such as strong acidic properties caused serious corrosion to reactor wall, pipelines, and valves, slow reaction rate, and difficulty in catalyst separation. Therefore, the homogeneous acid catalysts are not suitable for commercial biodiesel production. But it will appear as a suitable alternative to the reaction esterification rather than transesterification.

#### 2.4.2.2 Heterogeneous acid catalysts.

Heterogeneous acid catalysts are preferred over homogeneous catalysts because do not dissolve in the alcohol and feedstock. Thus, they can be separated easily by filtration and can be reused [29]. Several types of heterogeneous acid catalysts are catalyze the esterification of free fatty acids to biodiesel such as sulfonic acid-functionalized solids-both ion-exchange organic resins and inorganic support and inorganic metal-oxide based super acids [36]. The development of different types of heterogeneous acid catalysts has widened the choice of feedstock for biodiesel production at high FFA. The advantages of using heterogeneous acid catalysts for biodiesel production such as insensitive to FFA content in the oil, catalyzed esterification and transesterification simultaneously, easy catalyst recovery from reaction media, have potential to be recycled and regenerated, minimize the number of washing steps required, and less corrosion toward reactors wall, pipelines, and valves compared to homogeneous acid catalyst. Moreover, the main dars of commercializing these catalysts are high cost, complicated synthesis procedures, and extreme reaction conditions for transesterification such as high reaction and

temperature. In addition, excessive leaching of into the reaction mixture will contribute to the loss of active sites and decrease the reuse performances [37].

## **2.5 Factors affecting biodiesel production.**

The yield of biodiesel in transesterification is affected by several process parameters which following as; moisture and free fatty acids (FFA), reaction time, reaction temperature, catalyst and molar ratio of alcohol and oil [23].

### **2.5.1 Temperature**

Reaction temperature is affect the yield of biodiesel such as higher reaction temperature, increases the reaction rate and shortened the reaction time because the reduction in viscosity of oils but not exceed boiling point of alcohol in order to prevent the alcohol evaporation. However, the increase in the reaction temperature that exceeds the appropriate level will cause decrease of biodiesel yield, because higher reaction temperature accelerates the saponification and causes methanol to vaporize leads to decreased yield.

### **2.5.2 Reaction time**

The increase in fatty acid esters conversion when increase in reaction time. The reaction is slowly due to mixing and dispersion of reactant. After that the reaction proceeds very fast. In addition, longer reaction time bring about to the reduction of final product due to the reversible reaction of transesterification resulting in loss of esters as well as soap formation.

### **2.5.3 Methanol to oil molar ratio**

The stoichiometric ratio for transesterification must use 3 moles of methanol and 1 mole of oil. However, a high molar ratio is used to shift the chemical equilibrium toward the desired products due to the reversible reaction of transesterification. In addition, increasing the methanol-to-oil molar ratio increases the solubility, reduces the viscosity and increases the amount of contact between oil to alcohol. In consequence of biodiesel yield using methanol continuously increases with the raise of methanol molar ratio.

#### 2.5.4 Type and amount of catalyst

The most common catalyst are sodium hydroxide (NaOH) and potassium hydroxide (KOH). Further increasing concentration of catalysts lead to reduced biodiesel yield because the large amount of catalyst results in saponification and difficult separation of esters from glycerol and water. However, feedstock with high moisture and free fatty acids contents, homogenous transesterification process is unsuitable due to high possibility of saponification.

#### 2.5.5 Free fatty acid and water content

For the transesterification to give high yield, the alcohol should be free of moisture and the FFA content of the oil should be <0.5% [38]. The FFA and moisture contents have important effects on the transesterification of glycerides with alcohol. The high FFA content (>1% w/w) will happen soap formation and the separation difficult of products and hence, it has low yield of biodiesel product [39].

### 2.6 Spinning disk reactor (SDR)

Many reactors are currently use in the production of biodiesel. The spinning disk reactor is one of the interesting technology due to SDR provide the highest mixing efficiency. SDR is consist of a rotating disk within a stationary housing that uses centrifugal force to escape from the rotation of the disk. The disk has a liquid surface that will distribute into a thin film. The main structure of an SDR shows as Figure 8. The liquid enters at the disk center and flows speedily lateral as thin films on the disk surface. Compared to other reactors for biodiesel production, the SDR can obtained a high yield and production rate with a very short residence time [40]. In general, the limitations of biodiesel production are the resistance of mass transfer between oil and alcohol. Therefore, the response time is usually long when biodiesel is produced in a stirring tank due to its low mixing and mass transfer efficiency. The long reaction time decreases throughput or generate must increase reactor size [40].

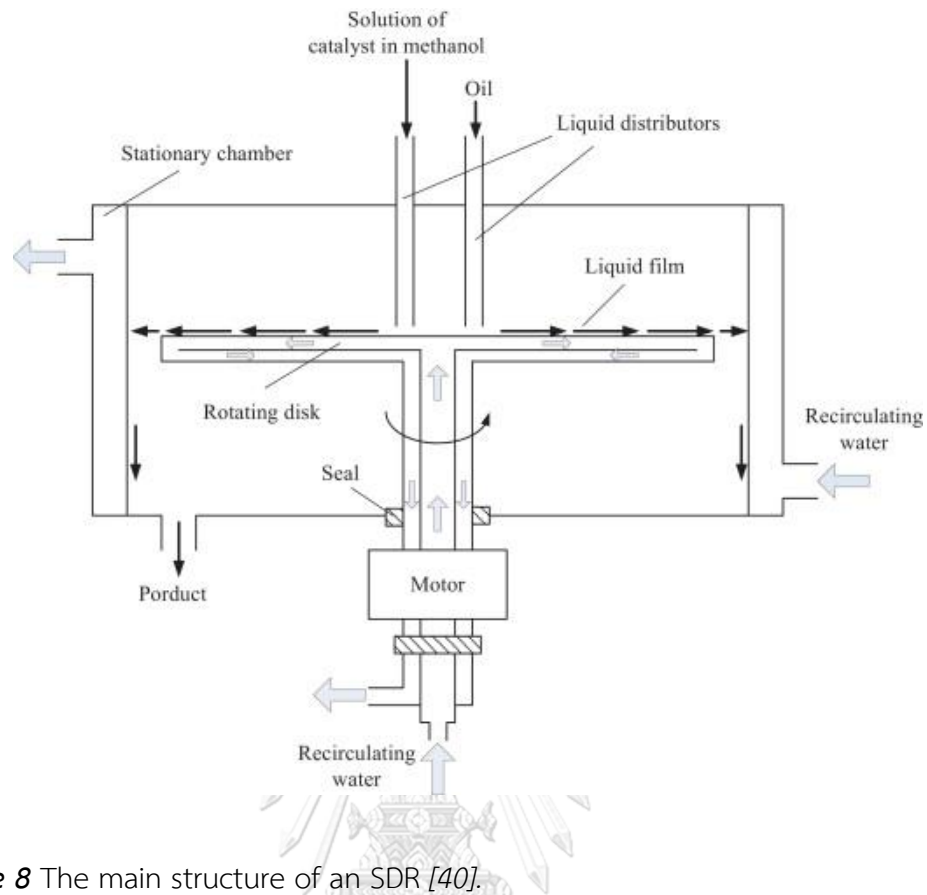


**Figure 8** The main structure of an SDR [40].

## 2.7 Design of experiment

Linear methods expose main effects and interactions but cannot find quadratic (or cubic) effects. Consequently, they have limitations in optimization. The optimum is found in some edge point consistent linear programming by Eq.(4). They cannot model nonlinear systems; e.g. quadratic phenomena [41]. When, nonlinearities are included in the design, the results provide an idea of the shape of the response surface are investigating. The methods are called response surface design (RSM). RSM are use in improve or optimal process settings in troubleshooting process problems. RSM is a technique effective with complex processes that make it easier to manage and explain results. In comparison with other methods [42].

$$Y = b_0 + b_1X_1 + b_2X_2 + b_{12}X_1X_2 + b_{11}X_1^2 + b_{22}X_2^2 \quad (4)$$

### 2.7.1 Central Composite Designs

Central Composite Design (CCD) has three different design points: edge points as in two level designs ( $\pm 1$ ), star points at  $\pm\alpha$ ;  $|\alpha| \geq 1$  (quadratic effects) and centre points. Central composite design type such as circumscribed (CCC), inscribed (CCI) and face centred (CCF) [41]. Show as Figure 9.

-Circumscribed (CCC) design is the original form of the central composite design. The star points are at some distance  $\alpha$  from the center depend on the properties desirous and the number of factors for the design.

- inscribed (CCI) the limits specified for factor settings are actually limits. The CCI design uses the factor settings as the star points and creates a factorial or fractional factorial design within those limits. CCI design also desires 5 levels of each factor.

- face centred (CCF) for CCF design the star points are at the center of each face of the factorial space, so  $\alpha = \pm 1$ . CCF design also requires 3 levels of each factor. Amplify an existing factorial or resolution V design with appropriate star points can also produce this design.

#### 2.7.1.1 Determining $\alpha$ in Central Composite Designs

The value of  $\alpha$  depends on the number of experimental runs in the factorial portion of the central composite design by Eq4:

$$\alpha = [\text{number of factorial run}]^{1/4} \quad (5)$$

If the factorial is a full factorial, then by Eq.5

$$\alpha = [2^k]^{1/4} \quad (6)$$

Values of  $\alpha$  depending on the number of factors in the factorial part of the design.

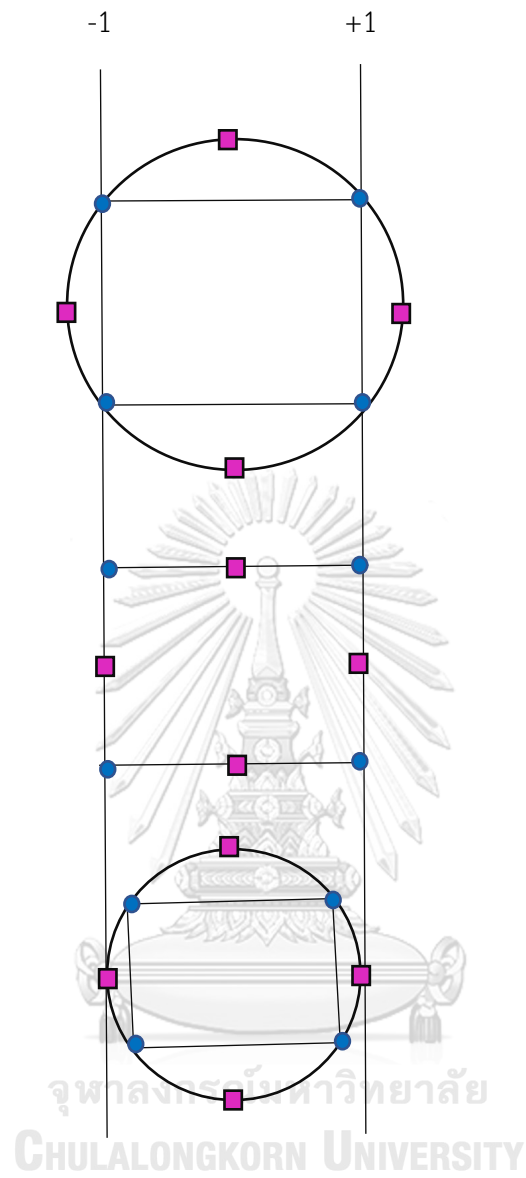


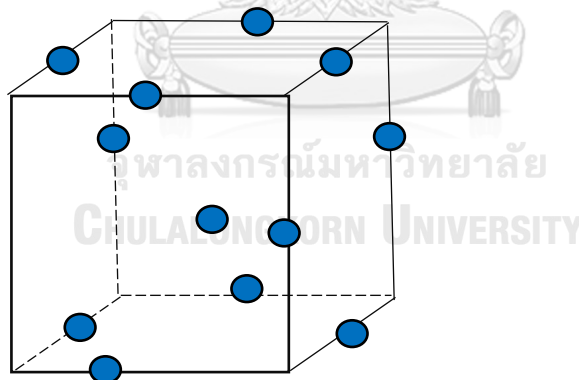
*Figure 9* Three types of central composite designs for two factors.

**Table 5** Values of  $\alpha$  as a function of the number of factors.

Number of Factors	Factorial Portion	Scaled Value for $\alpha$ Relative to $\pm 1$
2	$2^2$	$2^{2/4} = 1.414$
3	$2^3$	$2^{3/4} = 1.682$
4	$2^4$	$2^{4/4} = 2.000$
5	$2^{5-1}$	$2^{4/4} = 2.000$
5	$2^5$	$2^{5/4} = 2.378$
6	$2^{6-1}$	$2^{5/4} = 2.378$
6	$2^6$	$2^{6/4} = 2.828$

### 2.7.2 Box-Behnken designs

The Box-Behnken design is an independent quadratic design in that it does not contain an embedded factorial or fractional factorial design. For Box-Behnken design are at the midpoints of edges of the process space and at the center. These designs are rotatable and desire 3 levels of each factor. The designs have limited capability for orthogonal blocking compared to the central composite designs as shown in Figure 10.

**Figure 10** Three factors of Box-Behnken design.

The surface of the sphere bulge through each face with the surface of the sphere tangential to the midpoint of each edge of the space.



## Chapter 3

### Literature reviews

#### 3.1 Conventional process for biodiesel production

This chapter provides a brief overview of results reported in the literature on biodiesel production. Biodiesel fuel has benefits made it more attractive in recent times. It is known that the conventional technology involves the use of the conventional mechanical stirred reactor. Biodiesel is commonly produced by chemical transesterification. It can be produced from vegetable oils and animal fats using homogeneous (acid and alkaline) or heterogeneous catalysts. Homogeneous catalysts have been widely used for biodiesel due to their rather high catalytic activity and higher biodiesel conversion under mild conditions with high conversion in acceptable time. The impacts of catalyst types such as NaOH, KOH and CH<sub>3</sub>ONa on yield of biodiesel was studied by Leung et al. [43] reported that edible canola oil and used frying oil (UFO). This paper also studied the impacts of the physical and chemical properties of the feedstock oils and determined the optimal transesterification reaction conditions that produce the maximum ester content and yield. The optimal conditions found to be achieved at 60 °C for 20 min, 1.1 wt.% NaOH and 7:1 molar ratio of methanol/UFO. Keera et al. [44] studied the transesterification reaction of castor oil with homogeneous alkaline using batch reactor. The optimized conditions found to be 1 wt% KOH, 9:1 methanol to oil ratio and 60 °C reaction temperature for 30 min, the reaction mixture was continuously stirred at 400 rpm and providing a 95% FAME yield. Homogeneous catalysts have been widely used for biodiesel. But the process has some limitations, for example, produces soap as a side product, a large amount of water is wasted for the separation and cleaning of catalyst. To overcome these problems, including cost, which are effective, reusable, environmentally and do not produce much soap. Heterogeneous catalysts for the transesterification for favorable properties such as they are the least toxic material, cheap, easily available and have a low methanol solubility, higher activity and long catalyst lifetime. Many kind of catalyst have been studied by Kouzu et al. [45], CaO, Ca (OH)<sub>2</sub> and CaCO<sub>3</sub> were used as a solid

catalyst of biodiesel from soybean oil. At 1 h of reaction time, yield of FAME was 93% for CaO, 12% for  $\text{Ca}(\text{OH})_2$ , and 0% for  $\text{CaCO}_3$ . Demirbas [46] used CaO as a heterogeneous base catalyst from sunflower seed oil. Sunflower seed oil was subjected to the transesterification reaction. When the temperature was increased to 525 K, the transesterification reaction was essentially completed lead to within 6 min, 3 wt% CaO and 41:1 methanol/oil molar ratio. Studies the activity of activated CaO as a catalyst in the production of biodiesel by Granados et al. [47] CaO is one of the solids that have displayed higher activity for transesterification. Transesterification reaction of sunflower oil, using batch reactor 94% yield was achieved for 100 min at a temperature of 60 °C, using 3 wt% of the catalyst and methanol/oil molar ratio of 13:1.

Recently, researchers has considered systems included of CaO loaded on a carrier. Moreover,  $\text{CaO}/\gamma\text{-Al}_2\text{O}_3$  catalysts proved to be more active than oxides of other metals loaded onto  $\text{Al}_2\text{O}_3$ . Carrier supported CaO allows better dispersity such as greater availability of catalytically active sites, improved resistance to poisoning and better stability due to metal-carrier interactions. Based on Marinković et al. [1] report, loading CaO onto spherically-shaped  $\gamma\text{-Al}_2\text{O}_3$  support was applied for the preparation of a cost-effective and environmentally-friendly. The most active catalyst was derived from the nitrate precursor after calcination (475 °C). Reaction conditions (60 °C, 5 h, 900 rpm, methanol to oil molar ratio of 12:1 and catalyst loading (CaO wt% to the oil) of 0.5%). Yield of 94.3% was obtained in the methanolysis of sunflower oil in a three-neck round bottom glass reactor (250 mL). Zabeti et al. [8] reported that optimum catalyst activity for transesterification reaction was succeed by loading 100.54 wt.% of the calcium oxide precursor on alumina by calcination at 718 °C. The catalyst was reusable for two cycles. Transesterification the used of batch reactor for palm oil with methanol. The reports demonstrated that this catalytic activity can exhibited higher FAME yield by Pasupulety et al. [7] Transesterification were carried out in a 300 ml stainless steel Parr batch reactor. The catalysts studied the conversion of soybean oil to FAME formation was as follows:  $\text{CaO}/\text{neutral-}\text{Al}_2\text{O}_3 > \text{CaO}/\text{basic-}\text{Al}_2\text{O}_3 > \text{CaO}/\text{acidic-}\text{Al}_2\text{O}_3$ . 20%  $\text{CaO}/\gamma\text{-Al}_2\text{O}_3$  showed maximum biodiesel yield of mass 90% at 9:1

methanol/oil mole ratio.  $\text{Al}_2\text{O}_3$ -supported alkali and alkali earth metal oxides have been studied by Benjapornkulaphong et al. [48] Transesterification of palm kernel oil (PKO) and coconut oil (CCO) via the supported alkali metal catalysts,  $\text{LiNO}_3/\text{Al}_2\text{O}_3$ ,  $\text{NaNO}_3/\text{Al}_2\text{O}_3$  and  $\text{KNO}_3/\text{Al}_2\text{O}_3$  with active metal oxides formed, carried out in a 250-mL three-neck round bottom flask, showed very high methyl ester (ME) content (>93%) but  $\text{Ca}(\text{NO}_3)_2/\text{Al}_2\text{O}_3$  calcined at 450 °C yield of 94% with only a small loss of active oxides from the catalyst. The suitable condition of PKO and CCO over  $\text{Ca}(\text{NO}_3)_2/\text{Al}_2\text{O}_3$  are the methanol to oil molar ratio of 65, temperature of 60 °C and reaction time of 3 h, with 10 and 15–20% (w/w) catalyst to oil ratio for PKO and CCO, respectively. Besides, the combination of CaO with other oxide compounds in order to provide the higher catalytic activity has been widely studied. Mahdavi et al. [49] reported that biodiesel production from the transesterification using a 250 mL flask fitted with a stirrer of the cottonseed oil with ethanol was investigated over  $\text{CaO-MgO}/\text{Al}_2\text{O}_3$  catalyst. Catalysts were prepared via a conventional co-precipitation method. The optimized conditions predicted by Box–Behnken design were found to be 14.4 wt%  $\text{CaO-MgO}$  on  $\text{Al}_2\text{O}_3$ , molar ratio 12.24 and reaction temperature of 95.63 °C in order to achieve a conversion of 97.62%. On the other hand, the predicted results assent with the experimental results (12.5 wt% loading of  $\text{CaO-MgO}$  on  $\text{Al}_2\text{O}_3$ , molar ratio of 8.5 and reaction temperature of 95 °C with 92.45% conversion). Table 6 shows the research studies of conventional process using difference catalyst for biodiesel production. However, the main problem in biodiesel production process is the mass transfer between two immiscible reactants, resulting in a low process efficiency. Therefore, increasing the efficiency of mass transfer can help increase kinetic of the reaction and yield efficiency. Many researchers have studied intensification technologies for multiphase reactors to improve mixing [50].

**Table 6** Biodiesel production via different catalysts using conventional process.

Types of catalyst	Catalyst	Reaction conditions						Yield (%)	Reference
		Feedstock	Temperature (°C)	Methanol to oil molar ratio	Reaction time (h)	Catalyst loading (wt%)			
Homogeneous catalyst	NaOH	Rice bran oil	55	9:1	1	0.75	90	[51]	
	NaOH	Jatropha curcas seed oil	65	6:1	2	1.4	90	[52]	
	NaOH	Jatropha oil	65	6:1	1	1	73	[53]	
	KOH	Waste cooking oil	50	12:1	2	3	92.3	[54]	
	KOH	Waste cooking oil	70	6:1	1	1	98.2%	[55]	

Heterogeneous catalyst										
SrO metal oxide	Soybean oil	65	12:1	30min	3	95%	[33]			
CaO	Palm kernel shell biochar	65	9:1	4	3	99%	[56]			
CaO	Soybean oil	65	12:1	3	8	95%	[57]			
KOH/Al <sub>2</sub> O <sub>3</sub>	Waste cooking oil	70	9:1	2	15	96.8	[55]			
NaAlO <sub>2</sub> /γ-Al <sub>2</sub> O <sub>3</sub>	Palm oil	64.72	20.79:1	3	10.89	97.65%	[58]			
MgO/γ-Al <sub>2</sub> O <sub>3</sub>	Soybean oil	60	6:1	6	5	97%	[59]			
Ca/γ-Al <sub>2</sub> O <sub>3</sub>	Corn oil	65	12:1	5	6	87.89	[60]			
CaO/γ-Al <sub>2</sub> O <sub>3</sub>	Sunflower oil	60	12:1	5	0.5	94.3	[1]			

### 3.2 Intensification reactors for biodiesel production

The main problem in biodiesel production process is the mass transfer. In order to overcome these limitations of conventional techniques such as long reaction time, high molar ratio of alcohol to oil, catalyst concentration, high operating cost and energy consumption. Microwave irradiation has been used for biodiesel production. The chemical reactions are accelerated on account of selective absorption of microwave energy by polar molecules because the mixture of vegetable oil, alcohol, and catalyst, rapid heating occurs upon microwave irradiation. When the energy interacts with the reactant on a molecular level, very efficient heating is obtained. Instead, the conventional heating is slow and ineffective because transferring energy into a reactant depends upon convection currents and the thermal conductivity of the reaction mixture. Ding et al. [61] studied biodiesel production from palm oil using Microwave irradiation on transesterification reaction catalyzed by acidic imidazolium ionic liquids. A maximal yield of 98.93% was obtained while mole ratio of methanol to oil of 11, 9.17% of ionic liquid dosage of 9.17%, microwave power of 168 W and reaction 6.43 h. Microwave irradiation can be respected as an efficient process intensification method for biodiesel production. Effect to the capacity to short reaction time and save energy up to more than 44%. Lin et al. [62] reported that the reaction rate of transesterification, microwave radiation was used. The optimum conditions in microwave reactor were the molar ratio of 6, 1 wt% KOH, 200 rpm, and 65 °C. The conversion of the oil was 90% at reaction time 10 s. The reaction rate was much faster than that by the conventional heating method.

In addition, incorporating ultrasonic energy into conventional transesterification reactions can emulsify the reactants to reduce the requirement of catalyst amount, molar ratio, reaction time and reaction temperature. NaOH catalyzed transesterification was also studied by Georgogianni et al. [63]. The in situ transesterification with the use of ultrasonication and mechanical stirring led to similar high yields (95%) after approximately 20 min of reaction time. In the presence of ultrasonication lead to high ester yields (98%) in only 40 min of reaction time while use of mechanical stirring gave lower yields (88%) after 4 h when the reaction conditions were 2.0% NaOH, mechanical stirring (600 rpm) and methanol to oil molar

ratio 7:1. Micro-channel reactors achieve fast reaction rates by improving the efficiency of heat and mass transfer and apply high surface area/volume ratio and short diffusion distance. Wen et al. [50] reported that the zigzag micro-channel reactor with smaller channel size and more turns produces smaller droplets which result in higher efficiency of biodiesel production. Methyl ester yield of 99.5% at the residence time of only 28 s by using the zigzag micro-channel reactor at the mild reaction conditions: the molar ratio of methanol to oil of 9, the temperature of 56 °C, catalyst amount of 1.2 wt.%

In comparison between batch reactor to continuous reactor. Continuous reactor is offer better performance in improving heat and mass transfer, reduce cost for production, provide a uniform quality of the end- product, and support industrial-scale production. Table 7 shows as Types of reactor and performance of intensification method for biodiesel production. Thus, this article is review the development of current biodiesel production technologies and also to study the trend of techniques for biodiesel intensification such as spinning disk reactor.

**Table 7** Examples of biodiesel production processes via transesterification of oil using different variations of reactors.

Reactor	Catalyst	Reaction conditions						Yield (%)	Reference
		Feedstock	Temperature (°C)	Methanol to oil molar ratio	Reaction time (h)	Catalyst loading (wt%)			
Mechanical stirred reactor (MS)	CaO	Refined soybean oil	65	12:1	3	8	95%	[57]	
Continuous stirred tank reactor (CSTR)	CaO	rapeseed oil	60	10:1	2.5	2	90%	[64]	
Ultrasonic reactor	ostrich eggshell-derived CaO	Refined palm oil		9:1	1	8	92.7%	[65]	
High speed homogenizer	CaO	waste cooking oil	50	10:1	30 min	1	88%	[66]	



Reactor	Catalyst	Reaction conditions					Yield (%)	Reference
		Feedstock	Temperature (°C)	Methanol to oil molar ratio	Reaction time (h)	Catalyst loading (wt%)		
Microwave reactor	CaO/zeolite	waste lard	65	30:1	1.25	8%	90.89%	[67]
Fluidized bed reactor	whole-cell biocatalysts	waste cooking oil	35	3.74:1	48	10.21	91.8%	[68]
Zig-zag microchannel with zig-zag mixer	KOH	Soybean oil	59	8.5:1	14.9 s	1.17	99.5%	[69]
Spinning disk reactor (SDR)	KOH	Soybean oil	60	6:1	2-3 s	1.5	96.9%	[40]
Rotating packed bed reactor	K $\gamma$ -Al <sub>2</sub> O <sub>3</sub>	Refined soybean oil	60	24:1	1	7.05%	98.5	[70]

### 3.3 Spinning disc reactor for biodiesel production

The spinning disc reactor is an interesting technology. Currently, this type of reactor is widely used in production processes such as metallic iron nanoparticles [71], barium sulfate nanoparticles [72], precipitation [73], antipyrine removal [74], polymerization [75]. Biodiesel production process is an alternative to spinning disk reactor. The SDR reactor using fast reaction time which saves time in the work. Kai-Jie Chen et al. [40] reported that the continuous transesterification of soybean oil and methanol in a spinning disc reactor. Optimal yield of 96.9% was achieved with a residence time of 2–3 s (molar ratio of 6, KOH concentration of 1.5 %wt, temperature of 60 °C, flow rate of 773 mL/min and rotational speed of 2400 rpm). The production rate was high compared to other reactors for continuous transesterification process. SDR provided the highest mixing efficiency of several mixing appliances. SDR was achieved high yield and production rate with a very short residence time compared to other reactors. When, the high reaction temperature leads to excellent heat transfer efficiency. Rotating packed-bed reactor is another interesting process intensification technology due to the disc in the RPB designed to high centrifugal acceleration and increase mass transfer and micro mixing efficiencies [70]. Moreover, rotating packed bed reactor was high mixing rate achievable through the impingement process combined with the high shear forces associated with the fluid in contact with the disc surfaces, could provide the better mixing resulting to increase mass/heat transfer to obtain the reaction in a short residence time.

### 3.4 Rotating reactor for biodiesel production

For heterogeneous catalyst, vigorous mixing is essential to create enough contact amongst the three phases for transesterification. Moreover, higher dosage of the heterogeneous catalysts in slurry reactors increases the viscosity of the solution, leading to problems in mechanical mixing. So, rotating packed-bed reactor is another interesting process intensification technology due to the disc in the RPB designed to high centrifugal acceleration and increase mass transfer and micro mixing efficiencies by employing great centrifugal force, providing a good dispersion for a two-phase flow. Liquid flowing through the packing in the disc was generated to be the thin films. The RPB can intensify mass transfer and it has been widely used in many fields. Chen et al. [70] reported that biodiesel production using a RPB as a heterogeneously catalyzed transesterification reactor was represented a novel application of RPBs in the field of fuel production.  $K/\gamma\text{-Al}_2\text{O}_3$  catalyst packed in the rotator of the RPB. Activity of the  $K/\gamma\text{-Al}_2\text{O}_3$  catalyst would obviously decrease with the repetitive cycles due to the leaching of active species. The optimal conditions found to be achieved at 60 °C, molar ratios 24, void space of approximately  $0.638\text{ cm}^3/\text{cm}^3$  in the packed-bed rotator and a rotational speed of 900–1500 rpm are advantageous to the yield of fatty acid methyl esters (98.5%).

### 3.5 Mass transfer performance of rotating packed bed absorption

Enhance the performance of the RPB reactor, various rotors with different structures have been designed. The centrifugal acceleration can be produced thinner liquid film and tiny droplet with the contribution of packings and enhance the gas–liquid mass transfer. The RPB has an extensive applicability in a gas–liquid contacting processes such as absorption. Chang Lin et al. [76] reported that the mass transfer performance of the RPB with blade packings using VOCs absorption into water. Analyzing the gas-side mass-transfer coefficient and the effective gas–liquid interfacial area it was found that the enhancement in the effective gas–liquid interfacial area by the rotor speed was provided the contribution to the mass transfer by the centrifugal acceleration with the contribution of the blade packings for absorption. To reduce pressure drop of RPB equipped with random packing and structural designs used at higher gas flow rates for the gas adsorption process. Mass transfer performance was also studied by Chang Lin et al. [77]. This research has studied the effect of operating parameters on the mass transfer performance of RPB with blade packings for the absorption of CO<sub>2</sub> using MEA solution as shown in Figure 11, the arrangement of blade packing in RPB. The RPB with blade packings was used to remove CO<sub>2</sub> by chemical absorption using NaOH solution. The results study was showed that the RPB with blade packings has effective in removing CO<sub>2</sub> from exhaust gases. Therefore, the RPB with blade packings is excellent means of absorbing CO<sub>2</sub> with a high mass transfer.

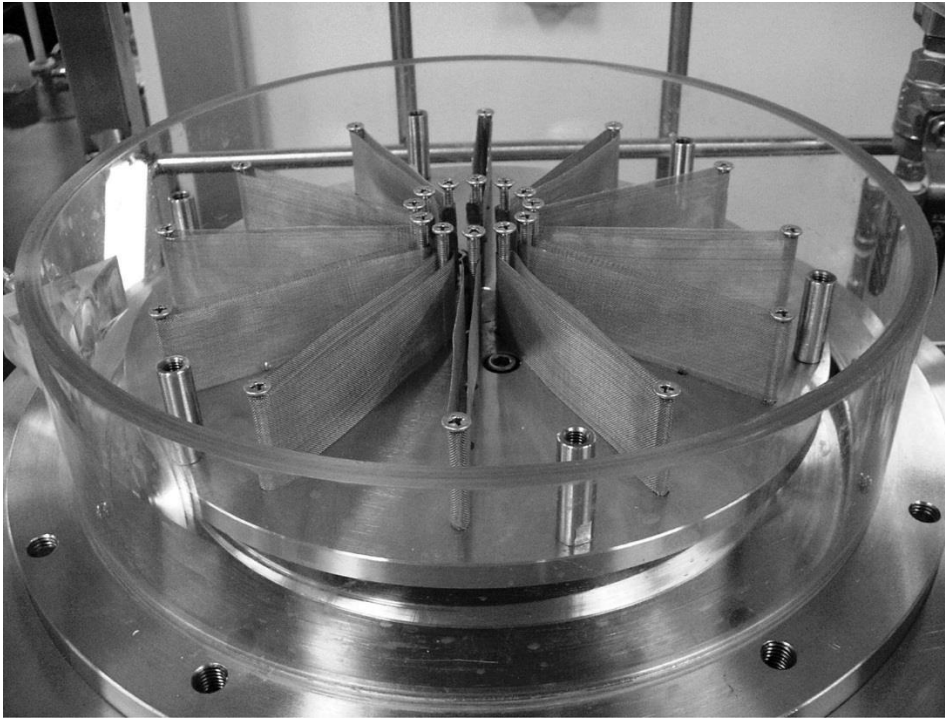


*Figure 11* RPB with blade packings.

### 3.6 Response surface methodology

Erewhile, the traditional one factor at a time (OFAT) method has been employed for optimizing the process. A traditional approach depended on only one factor at time by keeping another factors constant [78]. This method cannot study the interaction between factors. However, it is time-consuming, difficult, and economically unlikely because a large number of experiments to evaluate the optimal points [79]. To overcome these response surface methodology (RSM) is a multivariate statistical tool suitable for modeling the complex processes [80]. This tool is highly suitable when an experimental is affected by many variables and it can be applied to optimize the biodiesel production [81]. Applications of response surface methodology (RSM) and the central composite design (CCD) techniques to design and optimize of NaOH catalysts for the biodiesel production. Many researchers have been recently reported in the literature and their reliability to generate a model equation and to calculate optimum conditions have been proven. Zabeti et al. [8] studied the optimization of the activity of  $\text{CaO}/\text{Al}_2\text{O}_3$  catalyst for biodiesel production using response surface methodology. The reaction was carried out in a batch laboratory scale reactor. The

results showed that the calcination temperature and catalyst loaded on the support had significant effects on the biodiesel yield. The maximum basicity and biodiesel yield obtained were about 194  $\mu\text{mol/g}$  and 94%, respectively. The optimum condition was achieved by loading 100.54 wt.% of the calcium oxide precursor on alumina and calcination at 718 °C. The catalyst was reusable for 2 cycles. It can be seen that many researchers are interested in the study of CCD design. In which this researcher conducted a study on central composite rotatable design for startup optimization of anaerobic sequencing batch reactor treating biodiesel production wastewater. The experiment was considered three factors such as temperature (F1); inoculum mass, expressed as volatile suspended solids (F2) and reaction time (F3), in which this design had 5 levels. For this design, the number of runs is fifteen. Biodiesel production from used cooking oil using green solid catalyst was proposed by Tan et al. [82] The transesterification was optimized using a response surface methodology (RSM) based on three variables five level central composite design (CCD) as shown in Table 8 For the CCD design, 20 experimental runs were operated. The optimum condition was found to be 1.98%w/v of catalyst and alcohol/oil ratio of 10:1 at 65 °C in 1.54 h. The biodiesel yield of 89.5% was obtained under optimal conditions.

**Table 8** The 3- factors, 5- levels CCD optimizing the operating condition of transesterification.

Independent variables	Units	-1	0	+1	$-\alpha$	$+\alpha$
Catalyst concentration	%w/v	1	1.5	2	0.66	2.34
Temperature	°C	50	65	80	39.77	90.23
Time	h	1	1.5	2	0.66	2.34

## Chapter4

### Experimental

The experimental setups are divided into 3 parts. The first part is to study the preparation of  $\text{CaO}/\gamma\text{-Al}_2\text{O}_3$  catalyst and catalytic activity for the transesterification in a conventional mechanical stirred reactor for the preliminary work. The second part is to study the efficiency of the heterogeneous catalyst, it was adapted for use with RPB to find the optimum conditions for biodiesel production. In general, homogeneous catalytic systems are often used in spinning disc reactor but there are still drawbacks. The third part is adapted for the experimental design of response surface methodology (RSM) based on the central composite design (CCD) using homogeneous catalyst (NaOH) in RPB by packing inert packing bed.

#### 4.1 Chemicals

Cooking palm oil (CPO) was purchased from a local market in Thailand. Methanol employed in the reactions (>99.8% purity) was purchased from Thermo Fisher Scientific (Thailand), calcium nitrate tetrahydrate ( $\text{Ca}(\text{NO}_3)_2 \cdot 4\text{H}_2\text{O}$ ) (99%) was purchased from Sigma-Aldrich, sodium hydroxide (NaOH) pellets for analysis (>99.0%) was purchased from Sigma-Aldrich. The standards for FAME contained methyl esters (Methyl heptadecanoate > 99.0% purity) was purchased from Sigma-Aldrich. While Aluminum oxide (catalyst support, high surface area, gamma-phase, bimodal and 1/8" pellets) were purchased from Alfa Aesar (Thailand). n-Heptane ( $\text{CH}_3(\text{CH}_2)_5\text{CH}_3$ ) was purchased from Ajax Finechem (Thailand).

#### 4.2 Biodiesel production using heterogeneous catalyst

##### 4.2.1 Catalyst preparation

Catalysts were prepared by modified wet impregnation method of aqueous solution of calcium nitrate tetrahydrate on alumina support. The impregnation solution was prepared by  $\text{Ca}(\text{NO}_3)_2 \cdot 4\text{H}_2\text{O}$  equilibrium using 50%  $\text{Ca}(\text{NO}_3)_2 \cdot 4\text{H}_2\text{O}$  respect to the support mass in 50 mL of deionized water. In all cases, 8 g of  $\gamma$ -alumina in pellet form was dried at 120 °C for 24 h. After that,  $\gamma\text{-Al}_2\text{O}_3$  (8.0 g) was added to the impregnation

solution. The mixture was stirred for 2 h at room temperature. Subsequently, the excess water was heated overnight at 120 °C in an oven in order to remove water. All catalysts were calcined in N<sub>2</sub> atmosphere (10 L h<sup>-1</sup>) at temperature range from 400 to 700 °C for 4 h.

#### 4.2.2 Catalyst characterization

The synthesized CaO supported on  $\gamma$ -Al<sub>2</sub>O<sub>3</sub> catalyst was characterized using scanning electron microscope (SEM) and energy dispersive x-ray spectroscopy (EDS) to study the structure, shape and qualitatively or quantitatively characterize element. The x-ray diffraction (XRD) was carried out to study the crystalline structure of the materials and the phase identification were conducted using x-ray powder diffraction structural (XRPD) (D8 ADVANCE, BRUKER) analysis catalyst using Cu K $\alpha$  radiation ( $\lambda$  = 0.154178 nm) with a working voltage and current of 40 kV and 30 mA, respectively [36]. XRD data were collected in a range  $2\theta$  from 20 to 80 with slit width 0.6 mm at the scanning speed of 0.5 sec/step [70].

#### 4.2.3 Experimental setup in conventional mechanical stirred reactor

The biodiesel production was carried out by chemical transesterification using CPO as raw material and using CaO/  $\gamma$ -Al<sub>2</sub>O<sub>3</sub> as catalyst. Figure 12 displays the experimental setup of mechanical stirred reactor (MS), a 3-necked round bottom flask was equipped with a condenser circulated with cold water from an ice bath, a thermometer and a sampling valve as illustrated in the previous literature [83]. The reactions were performed using a stirrer speed of 900 rpm and temperature controlled at 60 °C by silicon oil bath. The methanolysis reaction was carried out in a 3-neck round bottom glass at 30 min. The reactor was immersed into a silicon oil bath. In all experiments, the reaction mixture was stirred at 900 rpm and the temperature at 60 °C. CPO was reacted with methanol in a molar ratio of 12:1. Catalyst loading were 3%wt (CaO of oil) for CaO/  $\gamma$ -Al<sub>2</sub>O<sub>3</sub>. The sample was taken every 15 min and quenched in an ice bath to stop the reaction. After that sample was centrifuged to remove the solid catalyst at rotational speed 3000 rpm for 5 min before analyzed by gas chromatography (GC).



In the case of catalyst reusability studies, the reaction condition was the same as previously described. Cooking palm oil was also reacted with methanol in a molar ratio of 12, catalyst loading was 3% wt (CaO of oil), reaction temperature of 60 °C and agitation speed of 900 rpm. The reaction mixture was removed from the reactor and the spent catalyst was recovered. After separation, the used catalyst was rinsed with methanol then the fresh palm oil and fresh methanol were filled in the reactor. The reaction time for each cycle was set up for 5 h.

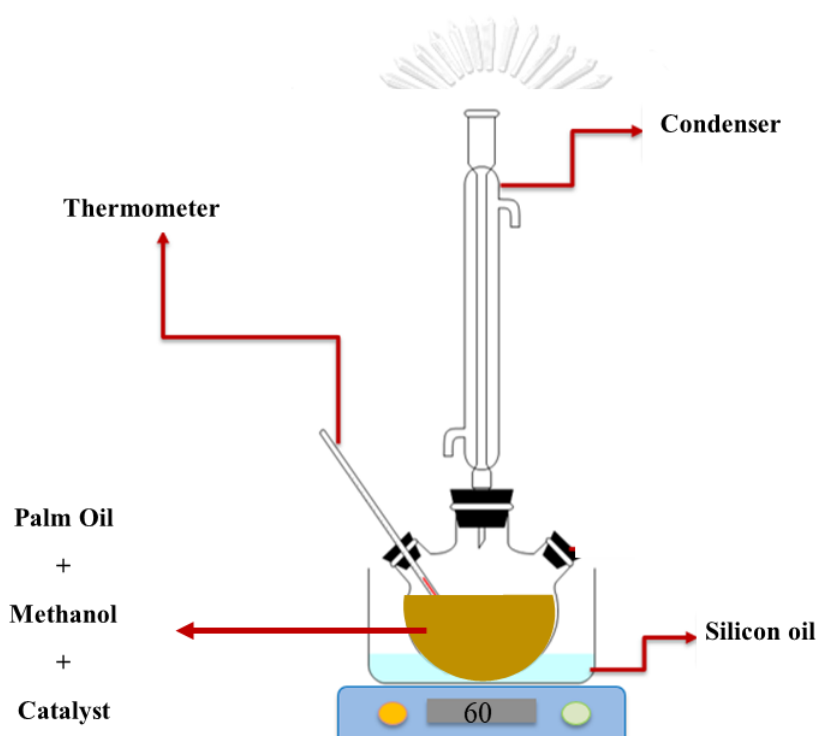


**Figure 12** Setup of conventional mechanical stirred reactor.

#### 4.2.4 Experimental setup in rotating packed reactor

The experimental setup of the RPB system shows as Figure 13 displays, which consists of RPB and a conventional mechanical stirred reactor (MS). Figure 14 is a simplified depiction of the RPB system. It has the radius and axial height of 15 and 0.6 cm, respectively. The MS was made of duran glass with volume of 1000 ml and equipped with a silicon oil bath to maintain a constant temperature. The design of the stirring speed was 800 rpm. A peristaltic pump (Model No:BT300N, shenchen) was used for the transport of the reaction solution. The total volume of the solution mixture

was 1000 ml for all experiments. The weight catalyst was set 40 g by packing in the packed-bed disc. The mixture was continuously circulated between the MS and RPB at a flow rate of 50-250 ml/min. The liquid feed were passed continuously over the packed bed rotating in the range of 500-2,000 rpm. The sample was taken every 30 min and quenched in an ice bath to stop the reaction. After that sample was centrifuged to remove the solid catalyst at rotational speed 3000 rpm for 30 min before analyzed by gas chromatography (GC).



*Figure 13* Set up of the RPB-MS reactor.

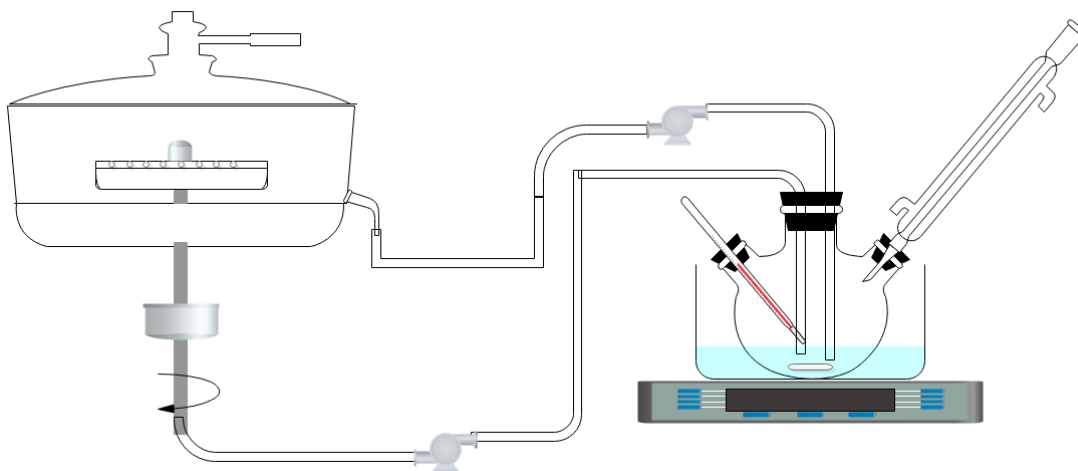


**Figure 14** Schematic of experimental RPB apparatus used for heterogeneously catalyzed transesterification reaction.

### 4.3 Biodiesel production using homogeneous catalyst in RPB

For biodiesel production using homogeneous catalysts, many researchers have studied in different reactors. The spinning disc reactor has been studied previously, used homogeneous catalyst effective of high biodiesel production compared to other reactors. However, the effect of inert packing bed on FAME yield has not been studied in RPB.

#### 4.3.1 Experimental set up

Figures 15 and 16 display the experimental setup of the RPB with inert bed packing, which consists of RPB, 3-necked round bottom flask and cylinder reactor tank. The cylinder reactor tank was used to preheat for CPO at 80 °C and a peristaltic pump was used for the transport of oil as can be seen in Figure 15 (a). The 3-necked flask was made of duran glass for reaction between methanol and NaOH at room temperature as illustrated in Figure 15 (b). The design of speed was 900 rpm for 3-necked flask. A peristaltic pump (Model No: BT300N, shenchen) was used for the transport of solution. Figure 15 (c) shows the RPB packed with inert bed on disc. The major parts were a stainless-steel disk driven by a motor. The equipment was installed with a 15 mm diameter disk rotating at 500-1,500 rpm. The inert packing bed as 3 mm

cylindrical of nylon ( 24.82 g) were packed in RPB. The reactant mixture was continuously flow at a flow rate of 130-390 ml/min. The reactant mixture were fed from the bottom of RPB onto the inside of disk and flows speedily outward. System temperature was controlled by recirculating hot water inside chamber from water bath show as Figure 15(d). A sample was taken every 20 min to assure a steady state condition at product tank (Figure 15(e)). After that sample was centrifuged to remove the glycerol and methanol at rotational speed 3000 rpm for 30 min, washed with water to obtain pure biodiesel and analyzed using GC analysis. The reactions were performed using temperature controlled at 60-65 °C by circulating hot water through the water bath. The energy consumption were measured by using a power plug-in meter for all experiments [84].

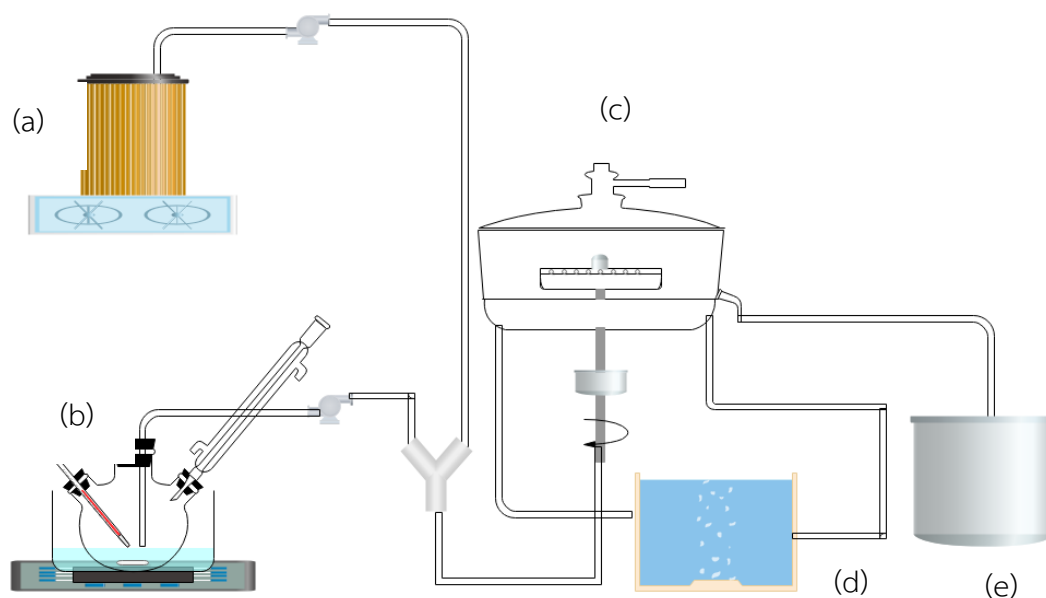


**Figure 15** Schematic of experimental RPB apparatus used for homogeneous catalyzed transesterification reaction.



*Figure 16* Setup of the RPB reactor.

#### 4.3.2 Design of experiments and optimization method.

Applications of central composite design (CCD) and response surface methodology (RSM) techniques to design and optimize the chemical have been reporting in the literature to generate a model equation and calculate optimum conditions [8]. In this work, the minitab (version 17) was used for the statistical design of experiments and data analysis by a three-level-four-factor CCD to investigate the effect of the parameters on biodiesel yield and to obtain a good model equation to predict the optimum conditions. The effect of the catalyst amount (A) (%), molar ratio of methanol to oil (B), rotational speed (C) (rpm) and flow rate (D) (ml/min) were considered.

#### 4.4 Analysis

The methyl esters yield was analyzed according to EN 14103 using a Perkin Elmer gas chromatography, equipped with a ZB5-HT capillary column (0.25 mm × 30 m). Helium was used as a carrier gas. The oven temperature ramp program was started from 150 °C and held for 5 min, 170 °C with a rate of 10 °C/min and held for 5 min, 220 °C with a rate of 3 °C/min. Temperatures of the injector and detector were 250 °C. Methyl ester yield was calculated by Eq. (7): [83].

$$\% \text{Yield} = \frac{(\sum A) - A_{EI}}{A_{EI}} \times \frac{C_{EI} \times V_{EI}}{m} \times 100\% \quad (7)$$

$\sum A$  is total peak area. (C14:0 – C24:1)

$A_{EI}$  is the peak area that corresponds to methyl heptadecanoate.

$C_{EI}$  is the concentration of the methyl heptadecanoate solution (mg/mL).

$V_{EI}$  is the volume of methyl heptadecanoate (mL).

$m$  is the mass of the biodiesel sample (mg).

#### 4.5 Yield efficiency calculation

The yield efficiency is calculated using Eq.8 [22] to compare the performance of different reactors (MS and RPB). It shows the amount of FAME produce per unit energy consume. The energy consumption is energy for mixing and heating [85]. In this study, the yield efficiency of different process intensification reactors were compared with RPB in order to find the most suitable reactor for biodiesel production.

$$\text{yield efficiency} = \frac{\text{Amount of product produced (g)}}{\text{Power supplied } \left(\frac{\text{J}}{\text{s}}\right) \times \text{reaction time (s)}} \quad (8)$$

## Chapter 5

### Results and discussion

The results and discussion are divided into 3 parts. The first part studies the preparation of (CaO/ $\gamma$ -Al<sub>2</sub>O<sub>3</sub>) catalyst and catalytic activity for the transesterification in a conventional mechanical stirrer reactor (MS). The second part studies biodiesel production in the presence of using CaO/ $\gamma$ -Al<sub>2</sub>O<sub>3</sub> heterogeneous catalysts using in RPB. The system was designed to increase mass transfer between two immiscible reactants which was expected to help increase kinetics of the reaction and yield efficiency. The third studies biodiesel production in the presence of NaOH homogeneous catalysts using RPB by packing inert packing bed. Therefore, the experiments were designed with the uses of RSM and CCD to find optimal conditions for biodiesel production.

#### 5.1 Biodiesel production in mechanical stirrer reactor using heterogeneous catalyst

##### 5.1.1 Catalyst characterization

##### 5.1.1.1 XRD studies

The XRD patterns of the support ( $\gamma$ -Al<sub>2</sub>O<sub>3</sub>) and catalysts obtained from nitrate precursor salts at different calcination temperatures are shown in Figure 17. The Al<sub>2</sub>O<sub>3</sub> support exhibits the characteristic reflections of  $\gamma$ -Al<sub>2</sub>O<sub>3</sub> at 37°, 39°, 46° and 67° which can be attributed to  $\gamma$ -Al<sub>2</sub>O<sub>3</sub> [6]. In the case of the catalysts obtained at the temperatures below 500 °C, there was the presence of precursor salt, Ca(NO<sub>3</sub>)<sub>2</sub> demonstrated by the peaks (2 $\theta$  of 26.51° and 41.32°) and 500 °C the 2 $\theta$  reflections disappeared. The results can be concluded that the nitrate precursor salt was completely decomposed in N<sub>2</sub> at around 500 °C. With increasing calcination temperature, the intensity of characteristic peak decreased and rarely appeared at higher temperatures. At the temperatures above 500 °C, the reflection related to CaO was identified. On the other hand, with CaO was identified according to its characteristic reflections (2 $\theta$  of 33.88°, 42.80° and 54.11°). The numbers of peak assigned to CaO increased and gained intensity but Baik et al. (1991) reported that the presence of CaO

inhibits the sintering of  $\text{Al}_2\text{O}_3$ . The reflection was related to  $\text{Ca}(\text{OH})_2$  at  $2\theta$  of  $28.9^\circ$  result from the adsorption of amount of moisture from the air in the measurement procedure [1].

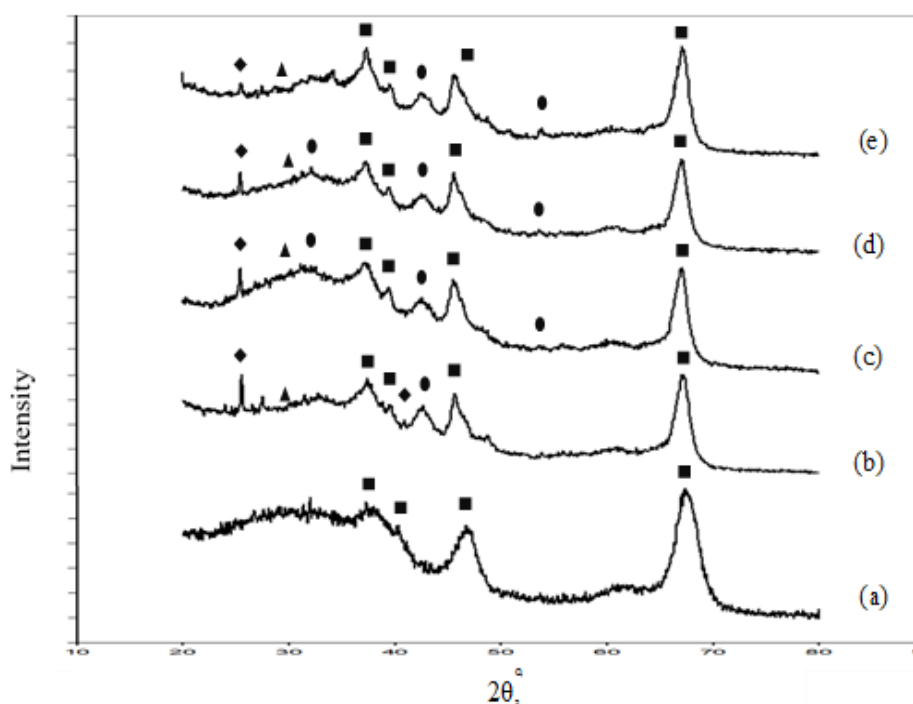


Figure 17 XRD patterns for samples (a)  $\gamma\text{-Al}_2\text{O}_3$ , catalysts obtained from the nitrate precursor; (b) 400 °C, (c) 500 °C, (d) 600 °C, (e) 700 °C; ■, ●, ▲, ◆ :  $\gamma\text{-Al}_2\text{O}_3$ , CaO,  $\text{Ca}(\text{OH})_2$  and  $\text{Ca}(\text{NO}_3)_2$ , respectively.

#### 5.1.1.2 SEM-EDS analysis

The scanning electron micrographs are presented in Figure 18 for the catalysts obtained from the nitrate precursor salt and calcined at 400, 500, 600 and 700 °C.  $\gamma\text{-Al}_2\text{O}_3$  support was exhibited a rod-like crystal structure of irregular orientation with the presence of sporadic agglomerates shown in Figure 18 (a). After loading CaO onto the support, only a group of structures with amorphous structured bunch was observed. The particle size was increased with increasing calcination temperature at the catalyst surface. The occurrence of agglomeration with increasing temperature from 400 to 600 °C as illustrated in Figures 18 (a-d) was obtained using the nitrate precursor. After calcination at 700 °C, amorphous-structured clusters disappeared because of possible



sintering as shown in Figure 18 (e) [1]. In addition, after loading CaO onto the support (Figure 18 (c)) of CaO/ $\gamma$ -Al<sub>2</sub>O<sub>3</sub> sample, it was indicated that Ca oxide particles were well deposited on the surface of  $\gamma$ -Al<sub>2</sub>O<sub>3</sub>, corresponding to 11.52 % according to EDS results. Figure 19 shows as the distribution of element on the surface of the catalyst at 500 °c can see that Ca is able to distribute well on the surface of the catalyst.

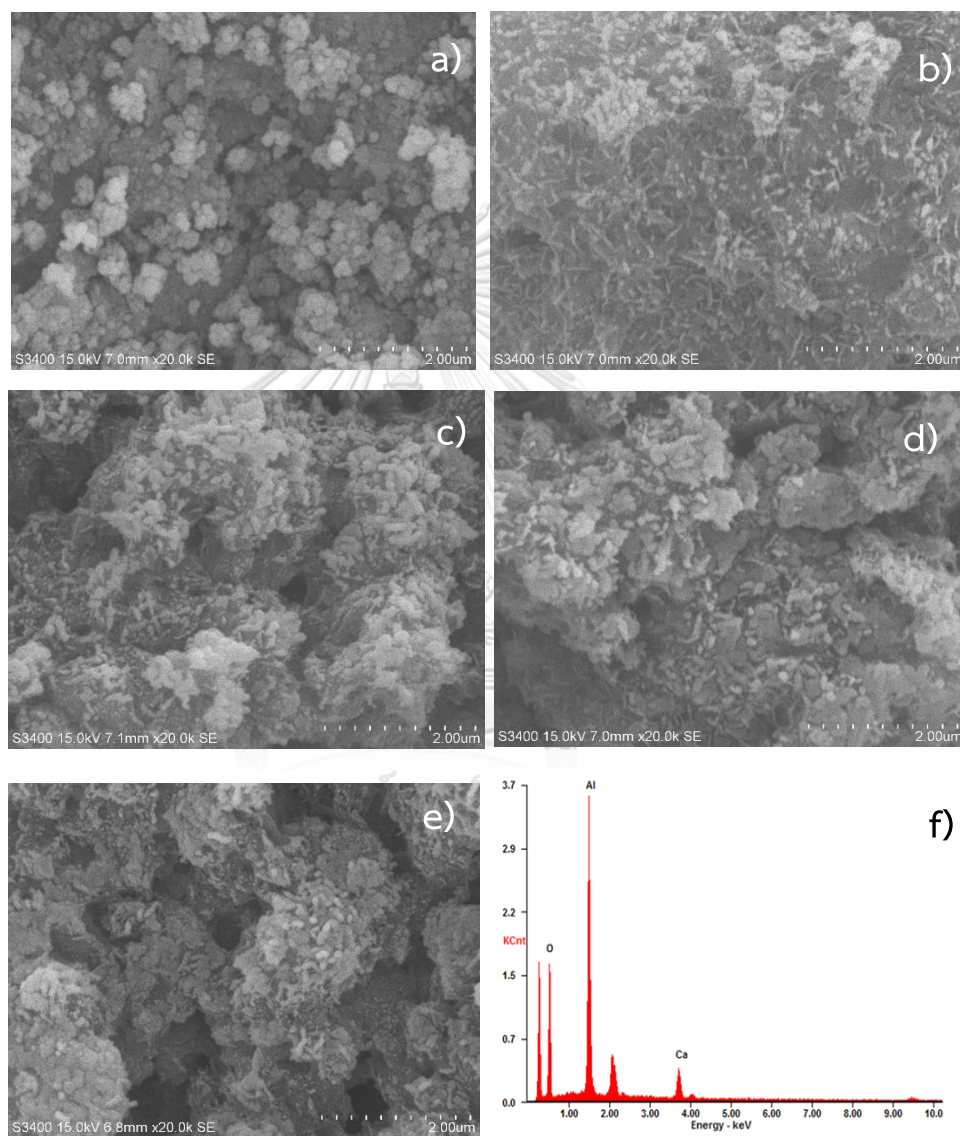


**Figure 18** SEM images of the catalyst carrier, support ( $\gamma$ -Al<sub>2</sub>O<sub>3</sub>) (a), catalyst derived from the nitrate precursor calcined at 400 °C (b), 500 °C (c), 600 °C (d) and 700 °C (e), respectively and EDS for 500 °C (f).

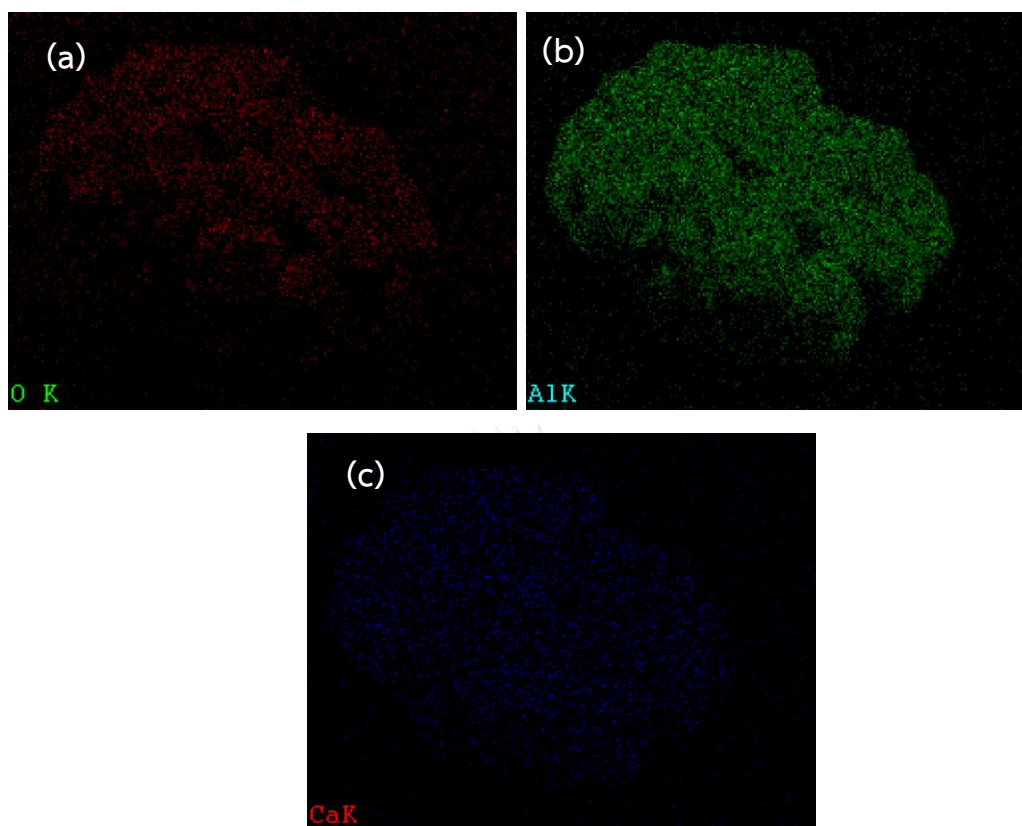


**Figure 19** EDS images of the CaO/ $\gamma$ -Al<sub>2</sub>O<sub>3</sub> catalyst at 500 °C.

#### 5.1.2 Effect of calcination temperature on FAME yield

Transesterification was employed for biodiesel production using conventional mechanical stirred reactor (MS) at a methanol-to-oil molar ratio of 12:1, catalyst loading of 0.5% wt CaO to oil and temperature of 60 °C. The CaO/ $\gamma$ -Al<sub>2</sub>O<sub>3</sub> catalysts were synthesized using the nitrate precursor salts and calcined at various temperatures. The effect of calcination temperature on FAME content was shown in Figure 20.

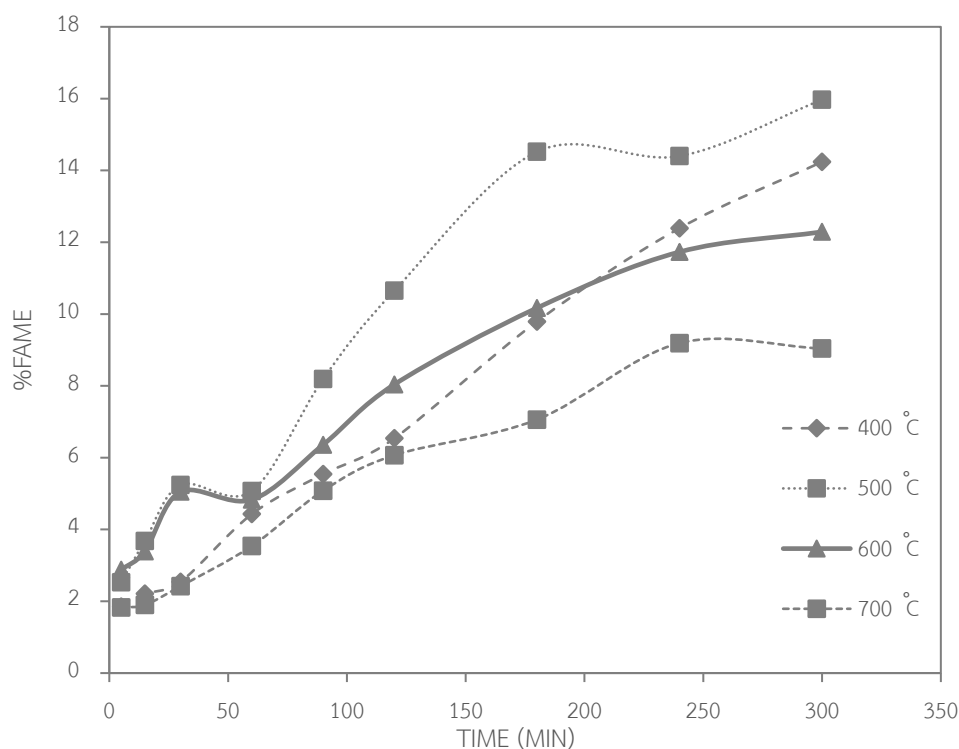


**Figure 20** The effect of calcination temperature on FAME yielded.

The catalytic activity of the  $\text{CaO}/\gamma\text{-Al}_2\text{O}_3$  catalysts depended on the calcination temperature. It was found that the FAME yield was increased with increasing of calcination temperature and the maximum yield was 15.97 % when using calcined catalyst at 500 °C. The observed change of the catalysts activity at different calcination temperatures were accorded with the results of the detailed textural, morphological and XRD analysis. In the case of this best performing catalyst, the nitrate precursor salt was completely decomposed into catalytically active species. However, the catalysts calcined at the highest temperatures did not show the highest activity, despite their very high content of catalytically active CaO as illustrated in Figure 17 (e). Reduced catalytic activity when calcined at higher temperatures was due to presence of catalytically inactive calcium aluminate and the agglomeration of the surface particles [1]. Figures 18 (b-e) show the results of SEM. It can be clearly seen that the distribution of active species was decreased as the high calcination temperature. Their smaller activity might be due to poor surface morphology promoted by the formation of larger CaO particles on the catalyst surface because of significant agglomeration at higher

temperatures [1]. Consequently, the most alkaline catalyst of nitrate precursor salts at 500 °C proved to be catalytically most active. At temperature (500 °C) catalytically inactive formed aluminates were not formed.

### 5.1.3 Effect of catalyst loading FAME yield

The effect of catalyst loading on FAME yield was investigated at 0.5 and 3%wt CaO to cooking palm oil. Transesterification was employed for biodiesel production using conventional mechanical stirred reactor (MS) and calcined catalyst at 500 °C as catalyst at a methanol-to-oil molar ratio of 12:1 and temperature of 60 °C. It is obvious that the influence of catalyst loading on FAME yield was significant. Figure 21 illustrates the obtained FAME yield at various catalyst loading. It can be clearly seen that an increase in catalyst loading from 0.5 to 3%wt resulted in an increase in the FAME yield from 16 to 58.06% at 5 h of reaction time. The reaction rate was only slightly higher at the initial time and taken a long time to reach equilibrium. With increasing catalyst loading, surface basicity and active surface increase. Therefore, the subsequent experiments for biodiesel production were based on the condition of a catalyst loading of 3 %wt CaO of oil.

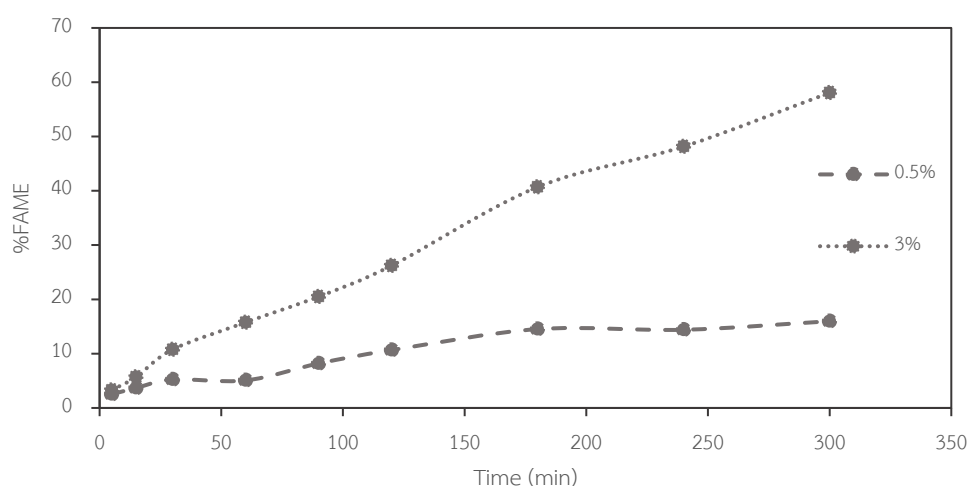


**Figure 21** Effect of catalyst loading on FAME yield. (molar ratios of 12, 0.5 - 3 % wt CaO to the oil and temperature of 60 °C).

#### 5.1.4 Effect of CaO loading on $\gamma$ -Al<sub>2</sub>O<sub>3</sub>

The effect of CaO loading on  $\gamma$ -Al<sub>2</sub>O<sub>3</sub> was investigated at 8, 12, 16, 20 and 24 %wt CaO loading on  $\gamma$ -Al<sub>2</sub>O<sub>3</sub>. Transesterification was employed via calcined catalyst at 500 °C as catalyst using conventional mechanical stirred reactor (MS) at a methanol-to-oil molar ratio of 12:1, catalyst loading of 3%wtCaO of oil and operating temperature of 60 °C. Figure 22 presents that CaO loading of the catalyst hugely affected the alkalinity and the catalytic activity. The CaO/ $\gamma$ -Al<sub>2</sub>O<sub>3</sub> catalyst with a CaO content of 24wt % exhibited the highest alkalinity and conversion. It can be clearly seen that an increase in CaO loading on  $\gamma$ -Al<sub>2</sub>O<sub>3</sub> from 12 to 24%wt resulted in increasing the FAME yield from 58.06 to 88.13% when compared with the reaction time of 90 min required for using 24%CaO/  $\gamma$ -Al<sub>2</sub>O<sub>3</sub> as catalyst.

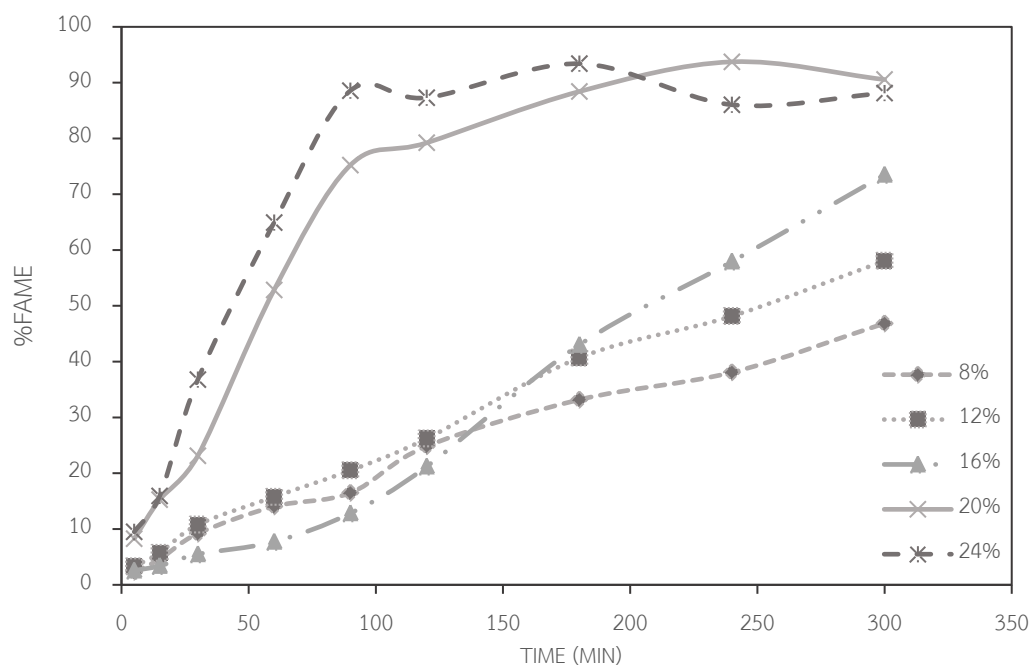


**Figure 22** Effect of CaO loading on  $\gamma$ -Al<sub>2</sub>O<sub>3</sub> (molar ratios of 12, 8 - 24 %CaO/ $\gamma$ -Al<sub>2</sub>O<sub>3</sub> and temperature of 60 °C).

#### 5.1.5 Evaluation of the catalyst reusability

The reusability experiments were studied for five consecutive cycles under reaction conditions: the catalyst loading of 3wt% CaO to the oil, methanol-to-oil molar ratio of 12:1, reaction temperature of 60 °C, stirrer speed of 900 rpm and reaction time at 5 h. After separation, the used catalyst was washed with methanol and no other

treatment was applied. Figure 23 shows the conversion achieved after different in consecutive batch cycles. High activity of the catalyst was achieved only in first to four cycles, where FAME yields were 88.73% and 78% after 5 h. At the fifth cycle, FAME yield dropped to 38.87% due to catalyst mechanical erosion caused by agitation. In addition, the deposition from the reaction mixture caused blocking of catalytically active sites on the surface of the catalyst [1].

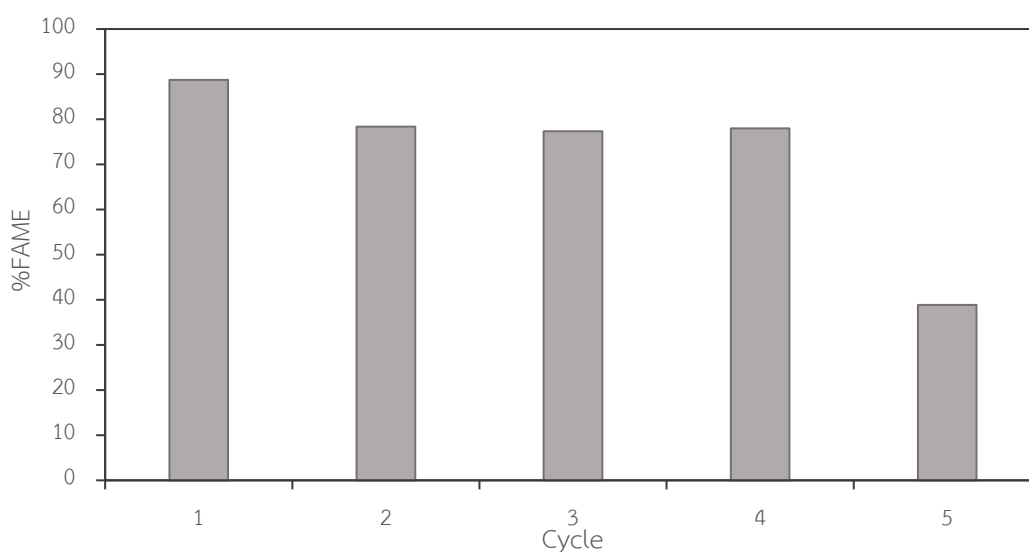


**Figure 23** The reusability of the  $\text{CaO}/\gamma\text{-Al}_2\text{O}_3$  catalyst without pretreatment in batch process.

The accumulation of organic molecules from the reaction mixture on the surface of the catalyst pellets resulted in a reduction of the total specific surface area of the catalyst by reducing the pore diameter [1].

## 5.2 Biodiesel production in rotating packed bed reactor using heterogeneous catalyst

In the previous studies, the suitable conditions were applied to the RPB reactors. The experimental conditions such as methanol-to-oil molar ratios (12) and reaction temperature (60 °C), rotational speed (1000 rpm), flow rate (250 mL/min) and reaction time (2 h) was carried out in RPB. The effect of the reaction time on the biodiesel yield is shown in Figure 24. It can be clearly seen that the longer the reaction time, the higher biodiesel yield. But, the yield of biodiesel production using RPB was

low compared to the MS reactor. Many researchers studying heterogeneous catalysts found that the oil conversion was particularly low initially. The conversion is heightened while the reaction time is extended. At extended reaction time to 120 min, the oil conversion is gently enhanced. When increasing reaction time to 150 min, a tiny increment is obtained indicating that the equilibrium point is reached within 120 min [55, 86]. It can be concluded that the time to achieve equilibrium was quite long for the heterogeneous catalyst. Therefore, it can indicate that the reaction time was not sufficiently long enough for using heterogeneous catalyst in RPB. Therefore, the RPB reactor is not suitable for biodiesel production via  $\text{CaO}/\gamma\text{-Al}_2\text{O}_3$  catalysts. The initially slow reaction is called the induction period. Induction period can be reduced in many ways such as supercritical process, intensification reactor and co-solvent method.

To further adapt this RPB reactor for biodiesel production, the experiments using homogeneous catalyst were conducted. Central composite design (CCD) design was used for designing experiment and finding the optimum conditions for the experiment for homogeneous catalyst in RPB reactor.

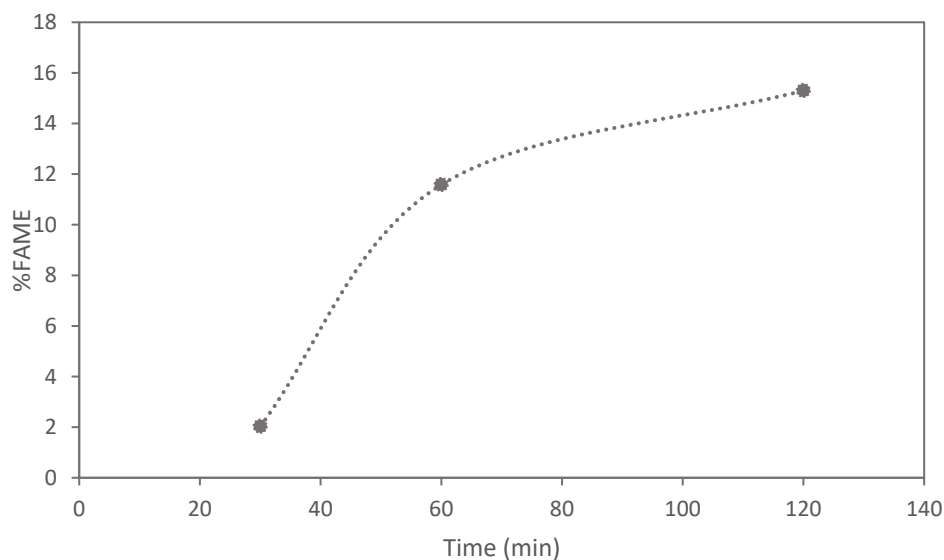


**Figure 24** Effect of reaction time for RPB reactor on biodiesel yield.

### 5.3 Biodiesel production in rotating reactor using homogeneous catalyst

From the previous results, the inert bed packing helps to distribute the flow of the reactants. By having liquid flow through the porous packing in the rotor, it could split the liquids into micro droplet or nano-droplet and thin films, and there is also an excellence renewed two-phase interface. Therefore, it is interesting to study the effect of inert packing bed which affects the production of biodiesel or FAME yield.

#### 5.3.1 Effect of inert packing bed

Previously, many researchers studied on the effect of different packing inert beds on fluid flow and improvement of mass transfer [14]. The results show that using inert bed can increase the efficiency of the mass transfer between two phases. In general, the inert packing bed was used in other systems such as distillation, absorption and reactive distillation [76, 87]. The effects of inert bed packing geometry, operating condition, and fluid property effect on mass transfer efficiency were reported [88]. For this research, the biodiesel production was studied in RPB with inert packing bed which is nylon hollow cylinder (height of 3 mm) and compared to the case without inert packing bed. Figure 25 shows the effect of inert packing bed on FAME yield in RPB under the condition of methanol to oil molar ratio of 6:1, NaOH catalyst amount of 0.5% wt of oil, flow rate of 260 ml/min and rotational speed of 1000 rpm at 60 °C. It can be clearly seen that an increase in reaction time from 10 to 20 minutes resulted in an increase in the FAME yield from 72.56 to 86.2% with using inert packing bed in RPB. It can be clearly seen that the use of inert packing bed offered higher biodiesel than the one without inert packing bed. The highest of fatty acid methyl esters (FAMES) was 88.21% for used inert packing bed in RPB. It can be concluded that the presence of the inert packing bed in RPB could increase the efficiency of mass transfer. The liquid film mass transfer depends on inert packing geometry, liquid properties, liquid flow, and gravity [88]. The liquid into the rotor of RPB was sheared by the porous packing, thus generating dispersion of the liquid and leading to the enhancement of mass transfer and micro-mixing. RPB was considered as a highly efficient contactor or reactor [89]. Mass transfer rate is crucial for an efficient column design in packed columns. Therefore, the study of liquid flow rate and rotational speed to explain the effect of mass transfer is important. The use of inert packing bed in RPB reactor affected



the production of biodiesel. Therefore, the CCD was used to design the experiments. Due to the above studies, the percentage of methyl esters did not meet the standards of ASTM and it was expected to use the CCD to find the optimum conditions for biodiesel production.

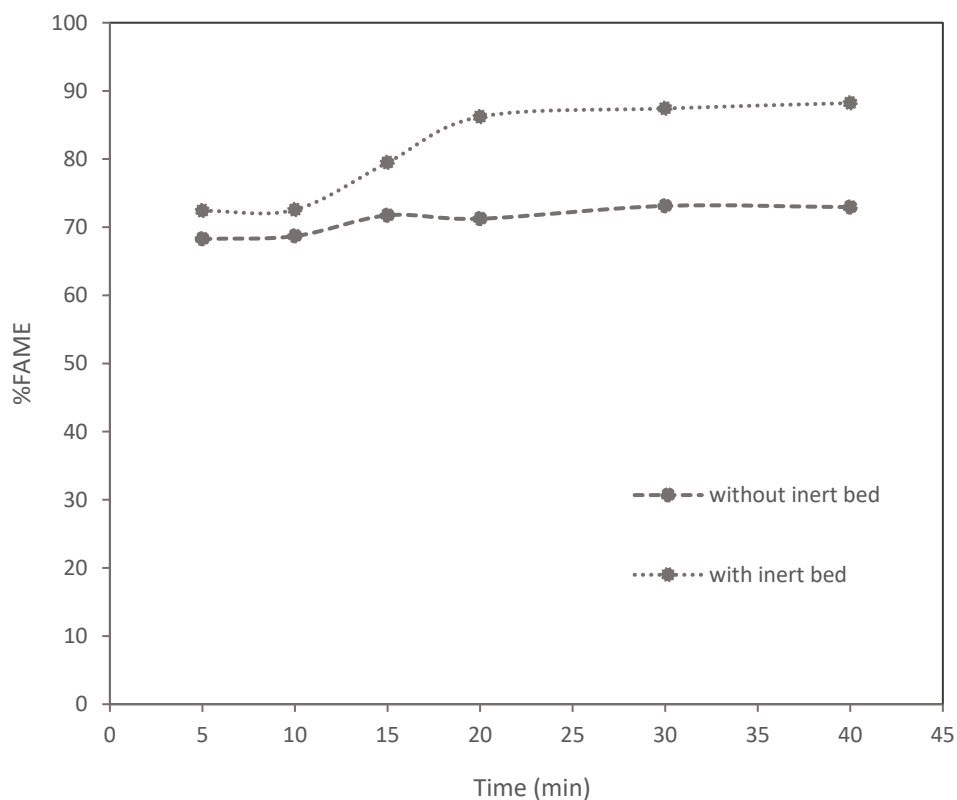


**Figure 25** Comparison of cases with inert packing bed of hollow cylinder and without inert bed packing on the transesterification.

### 5.3.2 CCD design

In this study, a 3-level and 4-factor CCD experimental design was applied to estimate the interaction between the variables and find the optimal condition for biodiesel yield. The effects of operation variables on the biodiesel yield such as catalyst amount (A), methanol to oil molar ratio (B), rotational speed (C) and flow rate (D) in the reaction process is present in Table 9. The coded values were defined by -1 (minimum), 0 (medium), +1 (maximum). Thirty-one experiments were reported from

the calculations for getting the experimental response of yield. All experiments were operated at 60 °C.

Four independent variables for biodiesel production were methanol to oil molar ratio (4.5:1–7.5:1), NaOH concentration (0.5–1.5 %wt), rotational speed (500–1500 rpm) and flow rate (130–390 ml/min). Table 10 presents the experimental runs performed and biodiesel yield obtained from each run.

**Table 9** Independent variables used for CCD in transesterification.

Variables	Symbol	Unit	Levels		
			-1	0	1
Catalyst amount	A	%	0.5	1	1.5
Molar ratio of methanol to oil	B		4.5	6	7.5
Rotational speed	C	rpm	500	1000	1500
Flow rate	D	ml/min	130	260	390

**Table 10** Experimental design conditions and experimental results of the responses.

Run	Factor1	Factor2	Factor3	Factor4	Response	
	A: Catalyst amount (%)	B: Molar ratio	C: speed (rpm)	D: Flow rate(ml/min)	Biodiesel yield (%)	
					Experimental	Predicted
1	0.5	4.5	500	130	66.83	66.70
2	1.5	4.5	500	130	87.1	86.37
3	0.5	7.5	500	130	57.73	62.59
4	1.5	7.5	500	130	84	85.54
5	0.5	4.5	1500	130	71.54	75.54
6	1.5	4.5	1500	130	98.77	96.49
7	0.5	7.5	1500	130	75.02	69.57
8	1.5	7.5	1500	130	86.01	93.80
9	0.5	4.5	500	390	73.07	70.86
10	1.5	4.5	500	390	78.96	80.99
11	0.5	7.5	500	390	66.81	65.67

Run	Factor1	Factor2	Factor3	Factor4	Response	
	A: Catalyst amount (%)	B: Molar ratio	C: speed (rpm)	D: Flow rate(ml/min)	Biodiesel yield (%)	
					Experimental	Predicted
12	1.5	7.5	500	390	77.5	79.07
13	0.5	4.5	1500	390	77.65	72.68
14	1.5	4.5	1500	390	83.4	84.09
15	0.5	7.5	1500	390	59.33	65.63
16	1.5	7.5	1500	390	83.6	80.31
17	0.5	6	1000	260	72.42	74.21
18	1.5	6	1000	260	94.72	91.38
19	1	4.5	1000	260	84.04	90.97
20	1	7.5	1000	260	95.53	87.03
21	1	6	500	260	91.35	87.47
22	1	6	1500	260	90.13	92.51
23	1	6	1000	130	98.39	92.27
24	1	6	1000	390	83.05	87.61
25	1	6	1000	260	89.45	91.49
26	1	6	1000	260	92.1	91.49
27	1	6	1000	260	87.21	91.49
28	1	6	1000	260	91.45	91.49
29	1	6	1000	260	90.2	91.49
30	1	6	1000	260	90.89	91.49
31	1	6	1000	260	89.97	91.49

Apart from that, response surface methodology (RSM) was used to investigate the effect of the four independent variables on the biodiesel yield as response variables.

### 5.3.3 Response surface methodology

The 3D response curves were drawn to show the effects of the independent variables on each other.

#### 5.2.3.1 Effect of catalyst amount

For this study, sodium hydroxide was used at three levels of 0.5, 1.0, and 1.5 wt%. Figure 26 shows the interaction effect of catalyst amount on FAME yield in RPB for CPO. It can be clearly seen that an increase in catalyst amount from 0.5 to 1 %wt resulted in an increase in the FAME yield because higher catalyst amount helps catalyze the reaction, resulting in higher biodiesel yield. On the other hand, it should be noted that the high excess catalyst amount (1.5% wt) can cause formation of OH groups and emulsions resulted in increased viscosity and reduced biodiesel yield [55]. The relationship between two independent variables (catalyst amount and the molar ratio of methanol to oil) and the effect on the response variable (Biodiesel yield) were considered. Biodiesel production increases as the catalyst amount increases. From Figures 26 (a) and (b), a trend of increase in biodiesel yield was observed with the increase of catalyst amount, molar ratio and rotational speed at first. However in Figure 26 (c), it can be seen clearly that the interaction between flow rate and catalyst amount has less effect compared to other variables on the biodiesel yield. Thus, the interaction effect of catalyst amount on the flow rate is inconsequential.

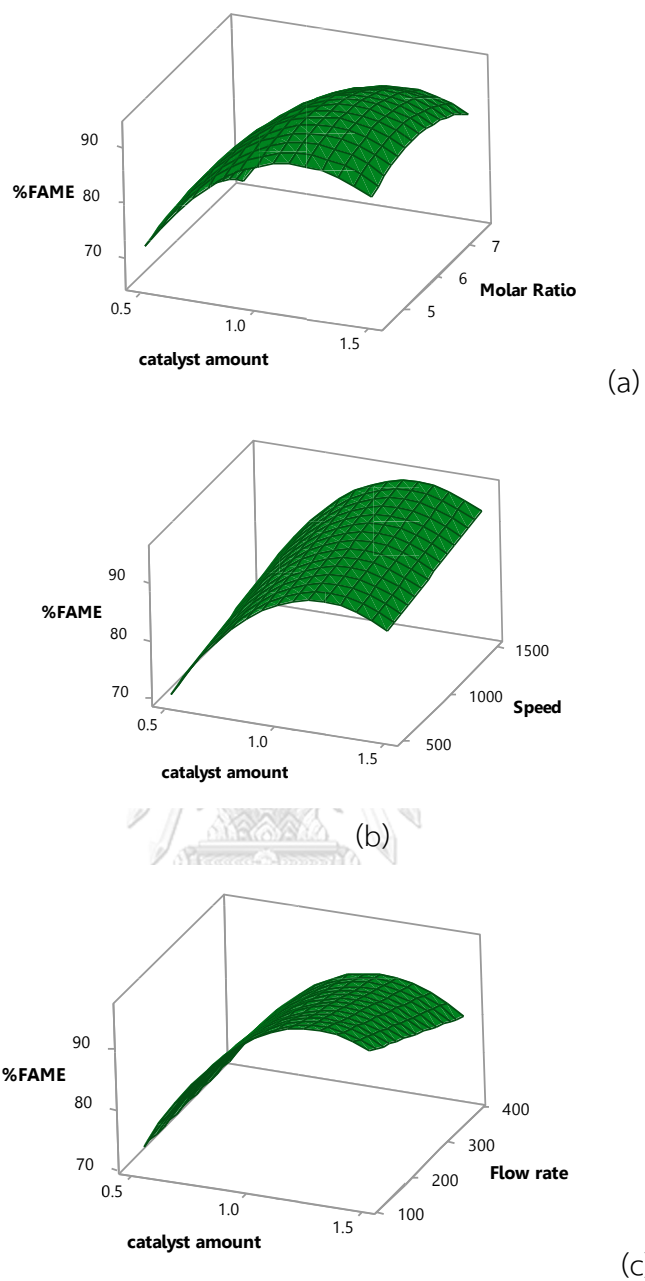


**Figure 26** 3D Plot of the interaction effects of (a) catalyst amount and molar ratio, (b) catalyst amount and rotational speed, (c) catalyst amount and flow rate on the transesterification.

The trend was reversed when the amount of catalysts reached a certain value approximately 1.2-1.3% as shown in Figures 26 (a-c). As the glycerol was formed with increasing amount of catalyst. Generally, a higher catalyst amount will lead to higher biodiesel conversion, but the excess catalyst will make esterification of free fatty acids progress faster and more water occurs in a shorter time. The excess water could deactivate the acidic hydroxyl groups as the hydration of these occur when water is generated [5]. The optimum of the catalyst amount was achieved at 1.27 %wt for biodiesel production within 20 min.

#### 5.3.3.2 Effect of methanol to oil molar ratio

The methanol to oil molar ratio is the most important parameters influencing the production of biodiesel. The effect of the methanol to oil molar ratio on the biodiesel yield was shown in Figures 27 (a) and (b). The methanol to oil molar ratio was investigated at three levels, including low level (4.5:1), middle level (6:1), and high level (7.5:1). The overall transesterification reaction was characterized by mass transfer, kinetic and equilibrium controls. The slowest one among these three stages is the mass transfer stage due to immiscibility of triglycerides and methanol [90]. The theoretical stoichiometry of biodiesel reaction for transesterification is 3 mol of biodiesel and 1 mol of glycerol to produced 1 mol of TG and 3 mol of methanol. Transesterification reaction is reversible. Therefore, a higher methanol to oil molar ratio is required to convert the reaction equilibrium to increase the contact between the immiscible methanol and triglyceride reactants [90]. Therefore, higher methanol to oil molar ratios give alkyl ester conversion in a shorter time [91]. Figure 27 shows the interaction effect of methanol to oil molar ratio on FAME yield in RPB. It can be clearly seen that an increase in methanol to oil molar ratio from 4.5 to 6 resulted in an increase in the FAME yield. Moreover, increasing methanol to oil increases biodiesel yield and biodiesel purity. According to studies, it has been found that increasing the methanol to oil molar ratio caused biodiesel yield increase. In addition, when increasing the methanol to oil molar ratio of 7.5 can be seen clearly that biodiesel production was decreased because excessive molar ratio causes a decrease in percentage yield. Theoretically, increasing the molar ratio of methanol to oil results in

the slower reaction because of the low oil concentration. The optimum methanol to oil molar ratio was achieved at 5.68 for biodiesel production within 20 min. Figure 27 (b) shows the effect of liquid flow rate. The results show that biodiesel yield increased slightly when increasing the flow rate of liquids from 130 to 260 ml/min. When comparing the relationship between molar ratio and flow rate, it can be seen clearly that the flow rate is not significant.

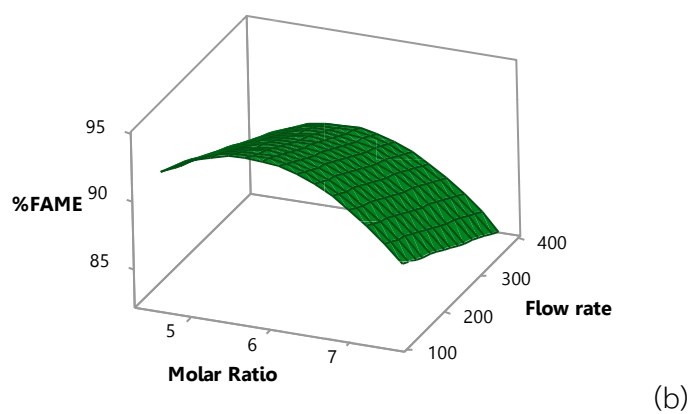
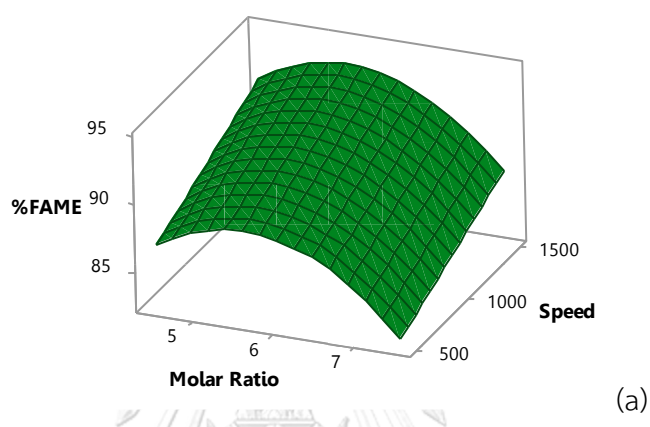


**Figure 27** 3D Plot of the interaction effects of (a) molar ratio and rotational speed, (b) molar ratio and flow rate on the transesterification.

### 5.3.3.3 Effect of rotational speed

Increasing yield may be due to improved mass transfer and the efficiency of micro-mixing by centrifugal force because a thin liquid film and flow rate are generated on the disk surface [40]. Increasing rotational speed provides a larger shear effect between liquid and inert packing bed, leading to the generation of tiny liquid units. It can generate a larger effective interfacial area and enhance the mass transfer [92]. In addition, increasing in the rotational speed is an increase of the relative movement of the liquid and packing and the hydrodynamic instabilities between two phase of liquid leading to enhanced shear effect and consequently smaller droplet diameter as the result of the droplet itself breaking up with an increasing rotational speed [89]. The high biodiesel yield can be obtained in RPB with a very short residence time. Increased biodiesel yield only slightly as rotational speed increased further to 1500 rpm because reduce residence time when rotational speed increase. The residence time can thus be controlled from the rotational speed, allowing combination of introducing high shear without losing residence time. To estimate the residence time of reactants on the disk following calculation Eq. 9 [40]. From the equation, it can be seen clearly that the flow rate and rotational speed increase, it decreases residence time of reactant according to this equation. The high shear stress is generated resulting in short diffusion path for reactants. The thickness of the diffusion is decreased by increased flow velocities in thin films modulated by rotational speed. This inverse relationship leads to shorter reaction times and more efficient reactions [93]. The shear force in the rotating disc depends primarily on the rotational speed, and the gap width between the disc. As the construction allows for very high tip speed and narrow gap width [94]. The RPB reactor with packing that the overall liquid holdup decreased with the increase of the rotational speed from 500 to 1500 rpm. From Fig. 27(a), the relationship between molar ratio and rotational speed, the higher the rotational speed, the higher the biodiesel yield because with the centrifugal force the liquid passing through the



inert bed was forced to distribute or split into very fine droplets and thin films by the high-shear forces [95].

$$\tau = \frac{3}{4} \left( \frac{12\pi^2\mu}{\rho Q^2 \omega^2} \right)^{1/3} (r_o^{4/3} - r_i^{4/3}) \quad (9)$$

where  $\mu$ ,  $Q$ ,  $\rho$ ,  $\omega$ ,  $r_i$  and  $r_o$  represent the viscosity of liquid (Pa.s), flow rate ( $\text{m}^3/\text{s}$ ), density of liquid ( $\text{kg}/\text{m}^3$ ), rotational speed (rad/s), radial position of the liquid distributor and disk radius, respectively.

#### 5.3.3.4 Effect of flow rate

An increase of liquid flow rate resulted in the increase of the number of droplet and the thickness of liquid film in the rotor [92]. The liquid was introduced into the RPB and dispersed into thin liquid films on the surface of the packing by the centrifugal force. For film structure for the liquid, the thickness of liquid film can be increased as the flow rate increased. Approximate analytical expression for the thickness of a liquid film on a rotating disc shows as Eq.10. From this equation, it can be seen clearly that increasing flow rate and/or decreasing speed result in a thicker film. However, increase of the liquid flow rate, the liquid velocity was increased leading to shorten the residence time. The different results from the turbulent of liquid flows in inert packing bed compared to the laminar flow of films. For the liquid flow rate and viscosity only effect mass transfer via the change of film thickness and the degree of liquid turbulence. The surface area for mass transfer is roughly equal to the surface area of the rotating disc and shear in the liquid film increase mass transfer. The residence time depends on flow rate of liquid on the disc, so that higher shear comes at shorter residence times. The inert bed is probably turbulent because of surface modification (embossing, holes, etc.) [88]. From Figures 26 (c) and 27 (b), it can be seen clearly that effect of flow rate on FAME yield in RPB for CPO. The results show that biodiesel yield increased slightly when increasing the flow rate of liquids from 130 to 260 ml/min. But when further increasing the flow rate to 390 ml/min, it did not affect the biodiesel yield. Figure 26 (c) exposed that less biodiesel yield and the interaction of variables

was low, while high catalyst amount indicate higher biodiesel yield. This result showed that increasing the flow rate did not increase the reaction conversion significantly.

$$h = \left( \frac{3\mu Q}{2\pi\rho r^2 \omega^2} \right)^{1/3} \quad (10)$$

where  $\mu$ ,  $Q$ ,  $\rho$ ,  $\omega$  and  $r$  represent the viscosity of liquid (Pa.s), flow rate (m<sup>3</sup>/s), density of liquid (kg/m<sup>3</sup>), rotational speed (rad/s) and disk radius, respectively.

### 5.3.3.5 Response analysis of variance

A second - order (quadratic) model was obtained to determine the biodiesel yield percentage expressed by Eq.11 as follows:

$$\begin{aligned} \text{Biodiesel yield} = & -19.8 + 88.5A + 11.9B + 0.0265C + 0.102D - 34.8 A^2 - 1.11 B^2 + 6 \times 10^6 C^2 \\ & - 9.2 \times 10^5 D^2 - 1.09 AB + 1.28 \times 10^3 AC - 0.0367 AD - 6.2 \times 10^4 BC - 1.4 \times 10^3 BD - 2.7 \times 10^5 CD \end{aligned} \quad (11)$$

where A, B, C and D are catalyst amount, methanol to oil molar ratio, rotational speed and flow rate. AB, AC, AD, BC, BD and CD are the interaction between the four independent variables. A<sup>2</sup>, B<sup>2</sup>, C<sup>2</sup> and D<sup>2</sup> are the squared terms. Figure 28 shows the values predicted by Equation (11) as compared with the experimental values of FAME. In biodiesel yield (%FAME) model, R<sup>2</sup> and R<sup>2</sup><sub>adj</sub> were 0.868 and 0.751, respectively.

Table 11 shows that the analysis of variance result provided a good prediction of the experimental result due to the probability value (p-value) for the model less than 0.0001 [82]. Consequently, it was proved that the model is statistically significant. The linear, square and 2-way interaction were used to measure effects on the biodiesel yield. The significance of each factor were estimated by the probability value (p-value) and Fisher's (F-Test). The high F-value or low the p-value shows the significant effects of those variables.

**Table 11** Analysis of variance for response surface quadratic model.

Source	Sum of squares	Degree of freedom (df)	Mean square	F-Value	P-Value
Model	3045.25	14	217.52	7.53	0.000
A - catalyst amount	1311.74	1	1311.74	45.39	0.000
B - Molar ratio	71.32	1	71.32	2.47	0.136
C - rotational speed	98.47	1	98.47	3.41	0.083
D - flow rate	98.09	1	98.09	3.39	0.084
AB	10.69	1	10.69	0.37	0.552
AC	1.64	1	1.64	0.06	0.815
AD	91.01	1	91.01	3.15	0.095
BC	3.50	1	3.50	0.12	0.732
BD	1.19	1	1.19	0.04	0.842
CD	49.14	1	49.14	1.70	0.211
A <sup>2</sup>	196.83	1	196.83	6.81	0.019
B <sup>2</sup>	16.14	1	16.14	0.56	0.466
C <sup>2</sup>	6.15	1	6.15	0.21	0.651
D <sup>2</sup>	6.31	1	6.31	0.22	0.647
Error	462.34	16			
Lack-of-Fit	447.14	10	44.71	17.65	0.001
Pure Error	15.2	6	2.53		
Total	3507.59	30			

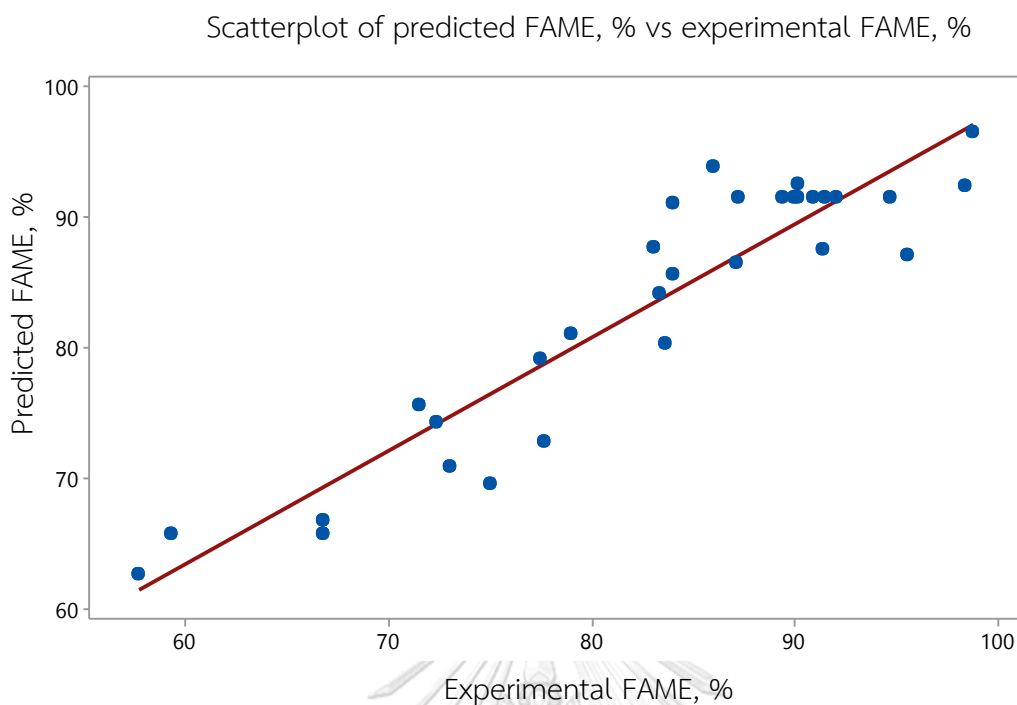


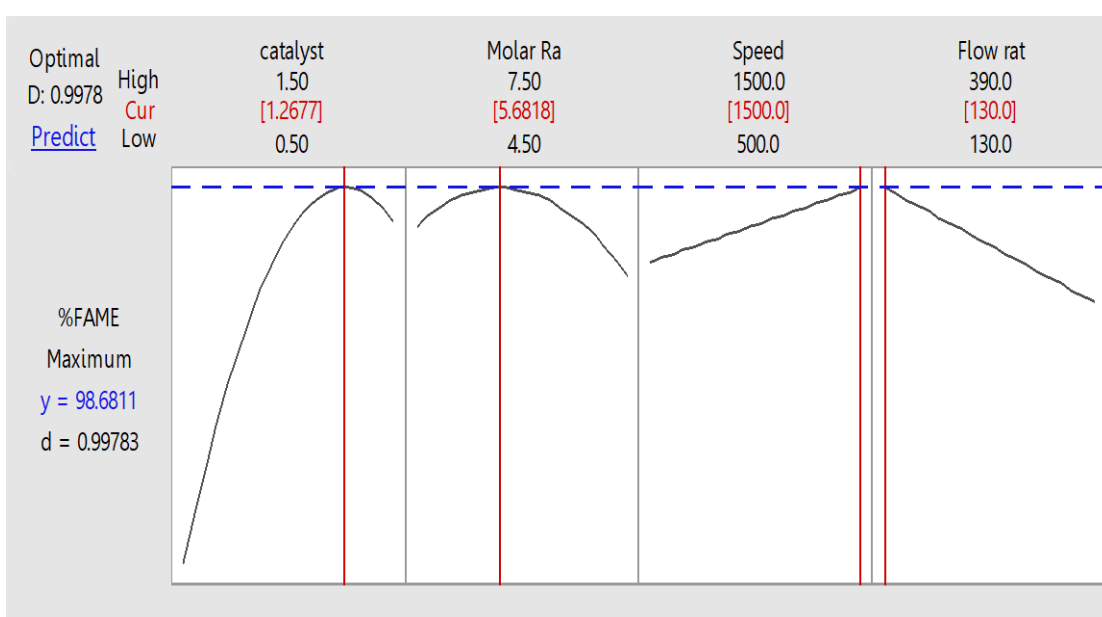
**Figure 28** Comparison of the experimental and predicted values of biodiesel yield.

#### 5.3.3.6 Optimization of response parameters

The optimization of response was operated to obtain the maximum biodiesel yield based on developed mathematical equations. The predicted response showed good agreement with the experimental results given in Table 12. Biodiesel yield at 98.68% were achieved with methanol to oil ratio (5.68:1) using NaOH as a catalyst (1.27% wt), rotational speed 1500 rpm and flow rate 130 ml/min in 20 minutes at 60 ° C. The results of optimization based on performance criterion was presented that the maximization of the oil conversion rate in Figure 29 corresponds to a minimum flow rate and a maximum of catalyst amount, molar ratio and rotational speed.

**Table 12** Optimization for maximum biodiesel yield.

Parameters	Optimized value
Catalyst amount	1.27
Molar ratio	5.68
Rotational speed	1500
Flow rate	130
%FAME	98.68

**Figure 29** Optimized results of response.

มหาวิทยาลัย  
CHULALONGKORN UNIVERSITY

#### 5.4 Performance comparison of different reactors on biodiesel yield

The yield efficiency was used to estimate the reactor performance based on energy usage, yield of biodiesel production and reaction time. The yield efficiency was used for consideration with other reactors with different mixing types. The measurement of total energy consumption included power input from each reactor. In addition, the performance of different reactors in term of yield efficiency is presented in Table 13. Yield efficiency was defined as the amount of product per unit energy required for the reaction. Appamana et al.(2019) [84] reported the highest biodiesel yield of 97.0% in a shorter reaction time of 2-3 s using spinning disc reactor under optimized conditions using a methanol to oil molar ratio of 6: 1, NaOH

concentration of 1.0 wt%, reaction temperature of 60°C, total flow rate of 260 ml min<sup>-1</sup> and rotational speed of 1,000 rpm. Kumar et al. (2019) reported that mechanical stirred (MS) was achieved 98.1% FAME yield after 25 min of reaction time under optimized conditions using 20 vol% methanol, 1.25 %wt KOH and reaction temperature of 150°C. Crudo et al. [96] reported the biodiesel production from refined palm oil using hydrodynamic cavitation of reaction time (10s). The highest biodiesel yield of 99%. In this study, the biodiesel yield as high as 98.77% was achieved with a very short residence time of 3.8s. Then, compares with previously reported methods. It can be seen clearly that reduction in the reaction time for the transesterification. When compared with conventional mechanical stirred reactor at reaction time of 90 min based on the similar conditions (temperature, amount of catalyst, rotational speed, flow rate and molar ratio of methanol to oil). RPBs has design to generate high centrifugal acceleration, providing a good dispersion for a two-phase flow due to enhancement effect on the transesterification to reduce mass transfer resistance.

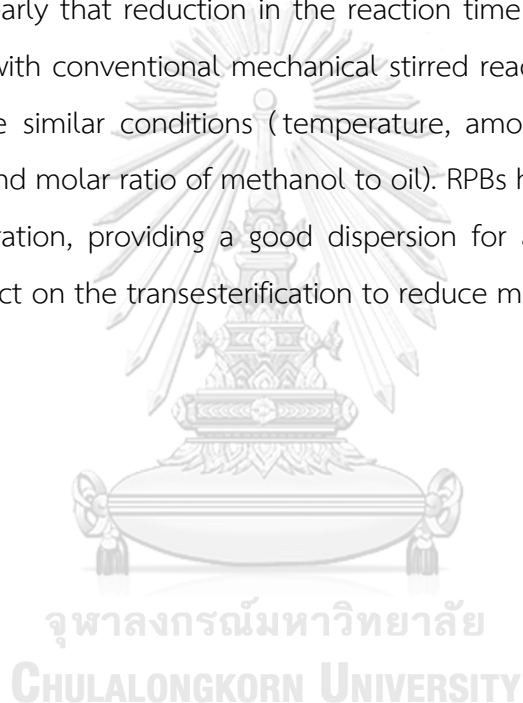


**Table 13** Comparison performance of RPB with other reactors with different mixing types (catalyst loading = 1%wt of oil and reaction temperature = 60 °C).

Reactor	Oil	Catalyst	Reaction time (min)	FAME yield (%)	Yield efficiency (g J <sup>-1</sup> )x10 <sup>-4</sup>	Reference
Mechanical stirred (MS)	Cooking palm oil	NaOH	90	97.7	1.6	This study
Rotating packed bed (RPB)	Cooking palm oil	NaOH	20 (τ=3.8s)	98.77	40.9	This study
Spinning disc (SDR)	Refined palm oil	NaOH	10 (τ<3s)	97	13.7	[84]
Hydrodynamic cavitation (HC)	Refined palm oil	NaOH	10 s	99	30	[96]
Mechanical stirred (MS)	Indian oil sardine fish	KOH	25	98.1	3.1	[97]

## Chapter 6

### Conclusions and recommendation

#### 6.1 Conclusions

The heterogeneous  $\text{CaO}/\gamma\text{-Al}_2\text{O}_3$  catalyst for biodiesel production from cooking palm oil by methanolysis was synthesized using modified wet impregnation method of aqueous solution of calcium nitrate tetrahydrate on alumina support. The calcination was under thermal activation in  $\text{N}_2$  at  $500\text{ }^\circ\text{C}$  for 4 h. The activated  $\text{CaO}/\gamma\text{-Al}_2\text{O}_3$  catalyst was in cylindrical shape with a diameter of 3 mm. The most active catalyst has morphological characteristics, enough developed surface area with cylindrical pores. In addition, the precursor was decomposed to CaO completely. It can be seen clearly that the maximum biodiesel yield of 90.24 % was achieved with the following optimum reaction conditions: the temperature of  $60\text{ }^\circ\text{C}$ , methanol-to-oil molar ratio of 12:1, 24% $\text{CaO}/\gamma\text{-Al}_2\text{O}_3$  catalyst loading of 3% wt (CaO of oil), stirring rate of 900 rpm and reaction time of 5 h. The  $\text{CaO}/\gamma\text{-Al}_2\text{O}_3$  catalyst maintained high activity only in the four batch cycles, after which its activity decreased in the fifth batch cycle.

The optimal conditions were applied to the RPB reactor but the result shown that, the yield of biodiesel was lower when compared to the MS reactor. It can be concluded that the required reaction time is quite long for the heterogeneous catalyst so the short residence time in the RPB was not sufficient for the operation using heterogeneous catalyst in RPB.

The inert packing bed helps to distribute the flow of the reactants by having liquid flowing through the inert packing bed in the rotor. The liquid into the rotor of RPB is sheared by the inert packing bed, thus generating dispersion of the liquid and leading to the enhancement of mass transfer and micro-mixing.

In addition, the producing biodiesel by homogeneous catalyst using RPB reactor was studied. The fatty acid methyl ester (FAME) yields as high as 98.68% could be achieved at a very short residence time of 3-4 s under the optimum condition: NaOH concentration of 1.27, methanol to oil molar ratio of 5.68, rotational speed of 1500 rpm and flow rate of 130 mL/min at  $60\text{ }^\circ\text{C}$  for 20 min. The use of statistical tool central



composite design can determine optimal values of variables for enhanced response by calculating correlation coefficient determination. The FAME content of the produced biodiesel could meet the ASTM standard. In addition, the yield efficiency of biodiesel production in RPB is higher than 25 times compared to MS. Therefore, RPB is a promising alternative reactor for continuous biodiesel production.

## 6.2 Recommendation

1. The presence of inert packing bed can enhance biodiesel yield because shear by the porous packing could help generate dispersion of the liquid, leading to the enhancement of mass transfer and micro-mixing. Therefore, the effect of inert packing bed shape or height should be also studied.

2. The effects of reaction temperature in the continuous process is an important parameter for the reaction. Therefore, it should be also studied to achieve higher performance.

3. Study induction period reduce for reaction in RPB reactor such as supercritical process, intensification reactor and co-solvent method.

4. Study the production of biodiesel with a RPB reactor at the same ratio of oil and catalyst compared to MS reactor.

## REFERENCES

1. Marinković, D.M., J.M. Avramović, M.V. Stanković, O.S. Stamenković, D.M. Jovanović, and V.B. Veljković, *Synthesis and characterization of spherically-shaped CaO/ $\gamma$ -Al<sub>2</sub>O<sub>3</sub> catalyst and its application in biodiesel production*. Energy Conversion and Management, 2017. **144**: p. 399-413.
2. Islam, A., Y.H. Taufiq-Yap, P. Ravindra, S.H. Teo, S. Sivasangar, and E.-S. Chan, *Biodiesel synthesis over millimetric  $\gamma$ -Al<sub>2</sub>O<sub>3</sub>/KI catalyst*. Energy, 2015. **89**: p. 965-973.
3. Lin, Y.-C., K.-H. Hsu, and J.-F. Lin, *Rapid palm-biodiesel production assisted by a microwave system and sodium methoxide catalyst*. Fuel, 2014. **115**: p. 306-311.
4. Azcan, N. and A. Danisman, *Alkali catalyzed transesterification of cottonseed oil by microwave irradiation*. Fuel, 2007. **86**(17): p. 2639-2644.
5. Narula, V., M.F. Khan, A. Negi, S. Kalra, A. Thakur, and S. Jain, *Low temperature optimization of biodiesel production from algal oil using CaO and CaO/Al<sub>2</sub>O<sub>3</sub> as catalyst by the application of response surface methodology*. Energy, 2017. **140**: p. 879-884.
6. Silveira Junior, E.G., V.H. Perez, I. Reyero, A. Serrano-Lotina, and O.R. Justo, *Biodiesel production from heterogeneous catalysts based K<sub>2</sub>CO<sub>3</sub> supported on extruded  $\gamma$ -Al<sub>2</sub>O<sub>3</sub>*. Fuel, 2019. **241**: p. 311-318.
7. Pasupulety, N., K. Gunda, Y. Liu, G.L. Rempel, and F.T.T. Ng, *Production of biodiesel from soybean oil on CaO/Al<sub>2</sub>O<sub>3</sub> solid base catalysts*. Applied Catalysis A: General, 2013. **452**: p. 189-202.
8. Zabeti, M., W.M.A.W. Daud, and M.K. Aroua, *Optimization of the activity of CaO/Al<sub>2</sub>O<sub>3</sub> catalyst for biodiesel production using response surface methodology*. Applied Catalysis A: General, 2009. **366**(1): p. 154-159.
9. Li, Z.-H., P.-H. Lin, J.C.S. Wu, Y.-T. Huang, K.-S. Lin, and K.C.W. Wu, *A stirring packed-bed reactor to enhance the esterification–transesterification in biodiesel production by lowering mass-transfer resistance*. Chemical Engineering Journal, 2013. **234**: p. 9-15.

10. Ge, D., Z. Zeng, M. Arowo, H. Zou, J. Chen, and L. Shao, *Degradation of methyl orange by ozone in the presence of ferrous and persulfate ions in a rotating packed bed*. *Chemosphere*, 2016. **146**: p. 413-418.
11. Chen, Y.-S., C.-C. Lin, and H.-S. Liu, *Mass Transfer in a Rotating Packed Bed with Various Radii of the Bed*. *Industrial & Engineering Chemistry Research - IND ENG CHEM RES*, 2005. **44**.
12. Jiao, W.Z., Y.Z. Liu, and G.S. Qi, *Gas Pressure Drop and Mass Transfer Characteristics in a Cross-flow Rotating Packed Bed with Porous Plate Packing*. *Industrial & Engineering Chemistry Research*, 2010. **49**(8): p. 3732-3740.
13. Wu, W., Y. Luo, G.-W. Chu, M.-J. Su, Y. Cai, H.-K. Zou, and J.-F. Chen, *Liquid flow behavior in a multiliquid-inlet rotating packed bed reactor with three-dimensional printed packing*. *Chemical Engineering Journal*, 2019.
14. Chu, G.-W., Y. Luo, Z.-Y. Xing, L. Sang, H.-K. Zou, L. Shao, and J.-F. Chen, *Mass-Transfer Studies in a Novel Multiliquid-Inlet Rotating Packed Bed*. *Industrial & Engineering Chemistry Research*, 2014. **53**(48): p. 18580-18584.
15. Kashyap, S.S., P.R. Gogate, and S.M. Joshi, *Ultrasound assisted synthesis of biodiesel from karanja oil by interesterification: Intensification studies and optimization using RSM*. *Ultrasonics Sonochemistry*, 2019. **50**: p. 36-45.
16. Demirbas, A., *Production of biodiesel fuels from linseed oil using methanol and ethanol in non-catalytic SCF conditions*. *Biomass and Bioenergy*, 2009. **33**(1): p. 113-118.
17. Tan, C.-P. and I.A. Nehdi, *13 - The Physicochemical Properties of Palm Oil and Its Components*, in *Palm Oil*, O.-M. Lai, C.-P. Tan, and C.C. Akoh, Editors. 2012, AOCS Press. p. 377-391.
18. Tan, C.P. and Y.B. Che Man, *Differential scanning calorimetric analysis of edible oils: Comparison of thermal properties and chemical composition*. *Journal of the American Oil Chemists' Society*, 2000. **77**(2): p. 143-155.
19. Firestone, D., *Physical and Chemical Characteristics of Oils, Fats, and Waxes (2nd Edition)*. AOCS Press. p. 4.
20. Joshi, R.M. and M.J. Pegg, *Flow properties of biodiesel fuel blends at low temperatures*. *Fuel*, 2007. **86**(1-2): p. 143-151.

21. Dai, Y.-M., J.-H. Lin, H.-C. Chen, and C.-C. Chen, *Potential of using ceramics wastes as a solid catalyst in biodiesel production*. Journal of the Taiwan Institute of Chemical Engineers, 2018. **91**: p. 427-433.
22. Chuah, L.F., S. Yusup, A.R. Abd Aziz, A. Bokhari, J.J. Klemeš, and M.Z. Abdullah, *Intensification of biodiesel synthesis from waste cooking oil (Palm Olein) in a Hydrodynamic Cavitation Reactor: Effect of operating parameters on methyl ester conversion*. Chemical Engineering and Processing: Process Intensification, 2015. **95**: p. 235-240.
23. Bozbas, K., *Biodiesel as an alternative motor fuel: Production and policies in the European Union*. Renewable and Sustainable Energy Reviews, 2008. **12**(2): p. 542-552.
24. <VegetableoilPropertiesUsesandBenefits.pdf>.
25. De Santi, V., F. Cardellini, L. Brinchi, and R. Germani, *Novel Brønsted acidic deep eutectic solvent as reaction media for esterification of carboxylic acid with alcohols*. Tetrahedron Letters, 2012. **53**(38): p. 5151-5155.
26. dos Santos, L.K., R.R. Hatanaka, J.E. de Oliveira, and D.L. Flumignan, *Production of biodiesel from crude palm oil by a sequential hydrolysis/esterification process using subcritical water*. Renewable Energy, 2019. **130**: p. 633-640.
27. Hájek, M. and F. Skopal, *Treatment of glycerol phase formed by biodiesel production*. Bioresource Technology, 2010. **101**(9): p. 3242-3245.
28. Hoekman, S.K., A. Broch, C. Robbins, E. Cenicerros, and M. Natarajan, *Review of biodiesel composition, properties, and specifications*. Renewable and Sustainable Energy Reviews, 2012. **16**(1): p. 143-169.
29. *Chapter 2. Vegetable Oil as a Fuel: Can it be used Directly?*, in *Biodiesel*. 2012. p. 5-30.
30. Lam, M.K. and K.T. Lee, *Chapter 15 - Production of Biodiesel Using Palm Oil*, in *Biofuels*, A. Pandey, et al., Editors. 2011, Academic Press: Amsterdam. p. 353-374.
31. Ali, O.M., R. Mamat, M.G. Rasul, and G. Najafi, *Chapter Eighteen - Potential of Biodiesel as Fuel for Diesel Engine*, in *Clean Energy for Sustainable*

- Development*, M.G. Rasul, A.k. Azad, and S.C. Sharma, Editors. 2017, Academic Press. p. 557-590.
32. Martinez-Guerra, E. and V.G. Gude, *Biodiesel production from vegetable oils: A sustainable energy alternative*. 2016. p. 55-82.
  33. Liu, X., H. He, Y. Wang, and S. Zhu, *Transesterification of soybean oil to biodiesel using SrO as a solid base catalyst*. *Catalysis Communications*, 2007. **8**(7): p. 1107-1111.
  34. Al-Widyan, M.I. and A.O. Al-Shyoukh, *Experimental evaluation of the transesterification of waste palm oil into biodiesel*. *Bioresource Technology*, 2002. **85**(3): p. 253-256.
  35. Kulkarni, M.G. and A.K. Dalai, *Waste Cooking Oil An Economical Source for Biodiesel: A Review*. *Industrial & Engineering Chemistry Research*, 2006. **45**(9): p. 2901-2913.
  36. Melero, J.A., J. Iglesias, and G. Morales, *Heterogeneous acid catalysts for biodiesel production: current status and future challenges*. *Green Chemistry*, 2009. **11**(9): p. 1285-1308.
  37. Lam, M.K., N.A. Jamalluddin, and K.T. Lee, *Chapter 23 - Production of Biodiesel Using Palm Oil*, in *Biofuels: Alternative Feedstocks and Conversion Processes for the Production of Liquid and Gaseous Biofuels (Second Edition)*, A. Pandey, et al., Editors. 2019, Academic Press. p. 539-574.
  38. <BF02541649.pdf>.
  39. Gashaw, A., T. Getachew, and A. Mohammed, *A review on biodiesel production as alternative fuel*. *J. For. Prod. Ind.*, 2015. **4**: p. 80-85.
  40. Chen, K.-J. and Y.-S. Chen, *Intensified production of biodiesel using a spinning disk reactor*. *Chemical Engineering and Processing: Process Intensification*, 2014. **78**: p. 67-72.
  41. <Introduction to Experiment Design\_2013.pdf>.
  42. <RSM.pdf>.

43. Leung, D.Y.C. and Y. Guo, *Transesterification of neat and used frying oil: Optimization for biodiesel production*. Fuel Processing Technology, 2006. **87**(10): p. 883-890.
44. Keera, S.T., S.M. El Sabagh, and A.R. Taman, *Castor oil biodiesel production and optimization*. Egyptian Journal of Petroleum, 2018. **27**(4): p. 979-984.
45. Kouzu, M., T. Kasuno, M. Tajika, Y. Sugimoto, S. Yamanaka, and J. Hidaka, *Calcium oxide as a solid base catalyst for transesterification of soybean oil and its application to biodiesel production*. Fuel, 2008. **87**(12): p. 2798-2806.
46. Demirbas, A., *Biodiesel from sunflower oil in supercritical methanol with calcium oxide*. Energy Conversion and Management, 2007. **48**(3): p. 937-941.
47. Granados, M.L., M.D.Z. Poves, D.M. Alonso, R. Mariscal, F.C. Galisteo, R. Moreno-Tost, . . . J.L.G. Fierro, *Biodiesel from sunflower oil by using activated calcium oxide*. Applied Catalysis B: Environmental, 2007. **73**(3-4): p. 317-326.
48. Benjapornkulaphong, S., C. Ngamcharussrivichai, and K. Bunyakiat, *Al<sub>2</sub>O<sub>3</sub>-supported alkali and alkali earth metal oxides for transesterification of palm kernel oil and coconut oil*. Chemical Engineering Journal, 2009. **145**(3): p. 468-474.
49. Mahdavi, V. and A. Monajemi, *Optimization of operational conditions for biodiesel production from cottonseed oil on CaO–MgO/Al<sub>2</sub>O<sub>3</sub> solid base catalysts*. Journal of the Taiwan Institute of Chemical Engineers, 2014. **45**(5): p. 2286-2292.
50. Nayak, M.G. and A.P. Vyas, *Optimization of microwave-assisted biodiesel production from Papaya oil using response surface methodology*. Renewable Energy, 2019. **138**: p. 18-28.
51. Sinha, S., A.K. Agarwal, and S. Garg, *Biodiesel development from rice bran oil: Transesterification process optimization and fuel characterization*. Energy Conversion and Management, 2008. **49**(5): p. 1248-1257.
52. Silitonga, A.S., H.H. Masjuki, T.M.I. Mahlia, H.C. Ong, A.E. Atabani, and W.T. Chong, *A global comparative review of biodiesel production from jatropha curcas using different homogeneous acid and alkaline catalysts: Study of physical and*

- chemical properties*. Renewable and Sustainable Energy Reviews, 2013. **24**: p. 514-533.
53. Tint Kywe, T. and M. Oo, *Production of Biodiesel from Jatropha Oil (Jatropha curcas) in Pilot Plant*. World Academy of Science, Engineering and Technology, 2009. **50**.
54. Mohod, A.V., P.R. Gogate, G. Viel, P. Firmino, and R. Giudici, *Intensification of biodiesel production using hydrodynamic cavitation based on high speed homogenizer*. Chemical Engineering Journal, 2017. **316**: p. 751-757.
55. Agarwal, M., G. Chauhan, S.P. Chaurasia, and K. Singh, *Study of catalytic behavior of KOH as homogeneous and heterogeneous catalyst for biodiesel production*. Journal of the Taiwan Institute of Chemical Engineers, 2012. **43**(1): p. 89-94.
56. Kostić, M.D., A. Bazargan, O.S. Stamenković, V.B. Veljković, and G. McKay, *Optimization and kinetics of sunflower oil methanolysis catalyzed by calcium oxide-based catalyst derived from palm kernel shell biochar*. Fuel, 2016. **163**: p. 304-313.
57. Liu, X., H. He, Y. Wang, S. Zhu, and X. Piao, *Transesterification of soybean oil to biodiesel using CaO as a solid base catalyst*. Fuel, 2008. **87**(2): p. 216-221.
58. Zhang, Y., S. Niu, C. Lu, Z. Gong, and X. Hu, *Catalytic performance of NaAlO<sub>2</sub>/V-Al<sub>2</sub>O<sub>3</sub> as heterogeneous nanocatalyst for biodiesel production: Optimization using response surface methodology*. Energy Conversion and Management, 2020. **203**: p. 112263.
59. Navas, M.B., I.D. Lick, P.A. Bolla, M.L. Casella, and J.F. Ruggera, *Transesterification of soybean and castor oil with methanol and butanol using heterogeneous basic catalysts to obtain biodiesel*. Chemical Engineering Science, 2018. **187**: p. 444-454.
60. Mohadesi, M., G. Moradi, and R. Rezaei, *Biodiesel Production using CaO/-Al<sub>2</sub>O<sub>3</sub> Catalyst Synthesized by Sol-Gel Method*. The Canadian Journal of Chemical Engineering, 2015. **93**.

61. Ding, H., W. Ye, Y. Wang, X. Wang, L. Li, D. Liu, . . . N. Ji, *Process intensification of transesterification for biodiesel production from palm oil: Microwave irradiation on transesterification reaction catalyzed by acidic imidazolium ionic liquids*. Energy, 2018. **144**: p. 957-967.
62. Lin, J.-J. and Y.-W. Chen, *Production of biodiesel by transesterification of Jatropha oil with microwave heating*. Journal of the Taiwan Institute of Chemical Engineers, 2017. **75**: p. 43-50.
63. Georgogianni, K.G., M.G. Kontominas, P.J. Pomonis, D. Avlonitis, and V. Gergis, *Conventional and in situ transesterification of sunflower seed oil for the production of biodiesel*. Fuel Processing Technology, 2008. **89**(5): p. 503-509.
64. Kouzu, M., A. Fujimori, R.-t. Fukakusa, N. Satomi, and S. Yahagi, *Continuous production of biodiesel by the CaO-catalyzed transesterification operated with continuously stirred tank reactor*. Fuel Processing Technology, 2018. **181**: p. 311-317.
65. Kumar, D., G. Kumar, Poonam, and C.P. Singh, *Ultrasonic-assisted transesterification of Jatropha curcus oil using solid catalyst, Na/SiO<sub>2</sub>*. Ultrason Sonochem, 2010. **17**(5): p. 839-44.
66. Joshi, S., P.R. Gogate, P.F. Moreira, and R. Giudici, *Intensification of biodiesel production from soybean oil and waste cooking oil in the presence of heterogeneous catalyst using high speed homogenizer*. Ultrasonics Sonochemistry, 2017. **39**: p. 645-653.
67. Lawan, I., Z.N. Garba, W. Zhou, M. Zhang, and Z. Yuan, *Synergies between the microwave reactor and CaO/zeolite catalyst in waste lard biodiesel production*. Renewable Energy, 2020. **145**: p. 2550-2560.
68. Chen, G., J. Liu, J. Yao, Y. Qi, and B. Yan, *Biodiesel production from waste cooking oil in a magnetically fluidized bed reactor using whole-cell biocatalysts*. Energy Conversion and Management, 2017. **138**: p. 556-564.
69. Dai, J.-Y., D.-Y. Li, Y.-C. Zhao, and Z.-L. Xiu, *Statistical Optimization for Biodiesel Production from Soybean Oil in a Microchannel Reactor*. Industrial & Engineering Chemistry Research, 2014. **53**(22): p. 9325-9330.



70. Chen, Y.-H., Y.-H. Huang, R.-H. Lin, N.-C. Shang, C.-Y. Chang, C.-C. Chang, . . . C.-Y. Hu, *Biodiesel production in a rotating packed bed using  $K/\gamma\text{-Al}_2\text{O}_3$  solid catalyst*. Journal of the Taiwan Institute of Chemical Engineers, 2011. **42**(6): p. 937-944.
71. Vilardi, G., M. Stoller, L. Di Palma, K. Boodhoo, and N. Verdone, *Metallic iron nanoparticles intensified production by spinning disk reactor: Optimization and fluid dynamics modelling*. Chemical Engineering and Processing - Process Intensification, 2019. **146**: p. 107683.
72. Bagheri Farahani, H., M. Shahrokhi, and A. Molaei Dehkordi, *Experimental investigation and process intensification of barium sulfate nanoparticles synthesis via a new double coaxial spinning disks reactor*. Chemical Engineering and Processing: Process Intensification, 2017. **115**: p. 11-22.
73. de Caprariis, B., M. Di Rita, M. Stoller, N. Verdone, and A. Chianese, *Reaction-precipitation by a spinning disc reactor: Influence of hydrodynamics on nanoparticles production*. Chemical Engineering Science, 2012. **76**: p. 73-80.
74. Expósito, A.J., D.A. Patterson, W.S.W. Mansor, J.M. Monteagudo, E. Emanuelsson, I. Sanmartín, and A. Durán, *Antipyrine removal by  $\text{TiO}_2$  photocatalysis based on spinning disc reactor technology*. Journal of Environmental Management, 2017. **187**: p. 504-512.
75. Boodhoo, K.V.K. and R.J. Jachuck, *Process intensification: spinning disc reactor for condensation polymerisation*. Green Chemistry, 2000. **2**(5): p. 235-244.
76. Lin, C.-C. and K.-S. Chien, *Mass-transfer performance of rotating packed beds equipped with blade packings in VOCs absorption into water*. Separation and Purification Technology, 2008. **63**(1): p. 138-144.
77. Lin, C.-C. and Y.-W. Kuo, *Mass transfer performance of rotating packed beds with blade packings in absorption of  $\text{CO}_2$  into MEA solution*. International Journal of Heat and Mass Transfer, 2016. **97**: p. 712-718.
78. Abou-Taleb, K.A. and G.F. Galal, *A comparative study between one-factor-at-a-time and minimum runs resolution-IV methods for enhancing the production of*

- polysaccharide by Stenotrophomonas daejeonensis and Pseudomonas geniculata*. *Annals of Agricultural Sciences*, 2018. **63**(2): p. 173-180.
79. Balajii, M. and S. Niju, *A novel biobased heterogeneous catalyst derived from Musa acuminata peduncle for biodiesel production – Process optimization using central composite design*. *Energy Conversion and Management*, 2019. **189**: p. 118-131.
80. Mäkelä, M., *Experimental design and response surface methodology in energy applications: A tutorial review*. *Energy Conversion and Management*, 2017. **151**: p. 630-640.
81. Bezerra, M.A., R.E. Santelli, E.P. Oliveira, L.S. Villar, and L.A. Escaleira, *Response surface methodology (RSM) as a tool for optimization in analytical chemistry*. *Talanta*, 2008. **76**(5): p. 965-977.
82. Tan, Y.H., M.O. Abdullah, J. Kansedo, N.M. Mubarak, Y.S. Chan, and C. Nolasco-Hipolito, *Biodiesel production from used cooking oil using green solid catalyst derived from calcined fusion waste chicken and fish bones*. *Renewable Energy*, 2019. **139**: p. 696-706.
83. Choedkiatsakul, I., K. Ngaosuwan, and S. Assabumrungrat, *Application of heterogeneous catalysts for transesterification of refined palm oil in ultrasound-assisted reactor*. *Fuel Processing Technology*, 2013. **111**: p. 22-28.
84. Appamana, W., P. Sukjarern, K. Ngaosuwan, and S. Assabumrungrat, *Intensification of Continuous Biodiesel Production Using a Spinning Disc Reactor*. *JOURNAL OF CHEMICAL ENGINEERING OF JAPAN*, 2019. **52**: p. 545-553.
85. Maddikeri, G.L., P.R. Gogate, and A.B. Pandit, *Intensified synthesis of biodiesel using hydrodynamic cavitation reactors based on the interesterification of waste cooking oil*. *Fuel*, 2014. **137**: p. 285-292.
86. Li, H., Y. Wang, X. Ma, Z. Wu, P. Cui, W. Lu, . . . Y. Wang, *A novel magnetic CaO-based catalyst synthesis and characterization: enhancing the catalytic activity and stability of CaO for biodiesel production*. *Chemical Engineering Journal*, 2019: p. 123549.
87. <Structured\_Packings.pdf>.

88. Song, D., A.F. Seibert, and G.T. Rochelle, *Mass Transfer Parameters for Packings: Effect of Viscosity*. Industrial & Engineering Chemistry Research, 2018. **57**(2): p. 718-729.
89. Sang, L., Y. Luo, G.-W. Chu, J.-P. Zhang, Y. Xiang, and J.-F. Chen, *Liquid flow pattern transition, droplet diameter and size distribution in the cavity zone of a rotating packed bed: A visual study*. Chemical Engineering Science, 2017. **158**: p. 429-438.
90. Musa, I.A., *The effects of alcohol to oil molar ratios and the type of alcohol on biodiesel production using transesterification process*. Egyptian Journal of Petroleum, 2016. **25**(1): p. 21-31.
91. Helwani, Z., M.R. Othman, N. Aziz, W.J.N. Fernando, and J. Kim, *Technologies for production of biodiesel focusing on green catalytic techniques: A review*. Fuel Processing Technology, 2009. **90**(12): p. 1502-1514.
92. Liu, W., G.-W. Chu, Y. Luo, Y.-Z. Liu, F.-Y. Meng, B.-C. Sun, and J.-F. Chen, *Mass transfer in a rotating packed bed reactor with a mesh-pin rotor: Modeling and experimental studies*. Chemical Engineering Journal, 2019. **369**: p. 600-610.
93. Sitepu, E.K., D.B. Jones, Y. Tang, S.C. Leterme, K. Heimann, W. Zhang, and C.L. Raston, *Continuous flow biodiesel production from wet microalgae using a hybrid thin film microfluidic platform*. Chemical Communications, 2018. **54**(85): p. 12085-12088.
94. Schilde, C., C. Mages-Sauter, A. Kwade, and H.P. Schuchmann, *Efficiency of different dispersing devices for dispersing nanosized silica and alumina*. Powder Technology, 2011. **207**(1): p. 353-361.
95. Liu, Y., Y. Luo, G.-W. Chu, F. Larachi, H.-K. Zou, and J.-F. Chen, *Liquid microflow inside the packing of a rotating packed bed reactor: Computational, observational and experimental studies*. Chemical Engineering Journal, 2019.
96. Crudo, D., V. Bosco, G. Cavaglia, G. Grillo, S. Mantegna, and G. Cravotto, *Biodiesel production process intensification using a rotor-stator type generator of hydrodynamic cavitation*. Ultrason Sonochem, 2016. **33**: p. 220-5.
97. Anand Kumar, S.A., G. Sakthinathan, R. Vignesh, J. Rajesh Banu, and A.a.H. Al-Muhtaseb, *Optimized transesterification reaction for efficient biodiesel*

*production using Indian oil sardine fish as feedstock.* Fuel, 2019. **253**: p. 921-929.



## Appendix A

### Residence time calculation

The residence time of reactants on the disk for RPB reactor was calculated using the following equation.

$$\tau = \frac{3}{4} \left( \frac{12\pi^2 \mu}{\rho Q^2 \omega^2} \right)^{1/3} (r_o^{4/3} - r_i^{4/3})$$

Q = reactant flow rate (m<sup>3</sup>/s)

$\rho$  = density of liquid (kg/m<sup>3</sup>)

$\mu$  = viscosity of liquid (Pa.s)

$\omega$  = rotational speed (rad/s)

r<sub>o</sub> = radius of the disk (m)

r<sub>i</sub> = radial position of the liquid distributor (m)

Example of calculation the reaction time

Total flow rate = 130 (ml / min)

Viscosity of palm oil = 88.6 × 10<sup>-3</sup> Pa.s

Density of liquid = 890.1 (kg / m<sup>3</sup>)

Radius of the disk = 0.075 m

Distance between liquid entering 2 positions = 0 m

Rotational speed = 1500 (rad / min)

$$\tau = \frac{3}{4} \left( \frac{12\pi^2 (88.6 \times 10^{-3})}{890.1 \times (2.17 \times 10^{-6})^2 \left(\frac{1500}{60}\right)^2} \right)^{1/3} \times (0.075^{4/3} - 0^{4/3})$$

$$\tau = 3.8 \text{ s}$$

## Appendix B

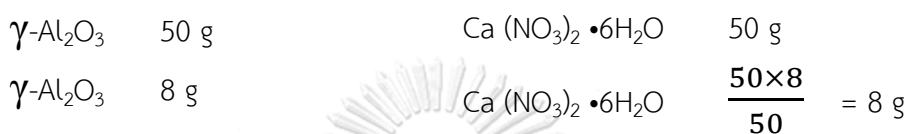
## Catalyst preparation

For example, 12%CaO/ $\gamma$ -Al<sub>2</sub>O<sub>3</sub>

Calcium nitrate hexahydrate 50 wt%

$\gamma$ -Al<sub>2</sub>O<sub>3</sub> (8.0 g)

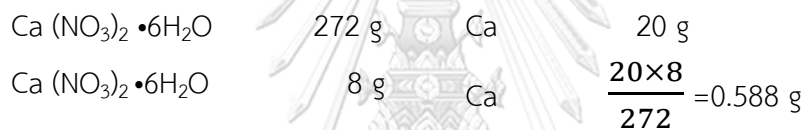
At first step,



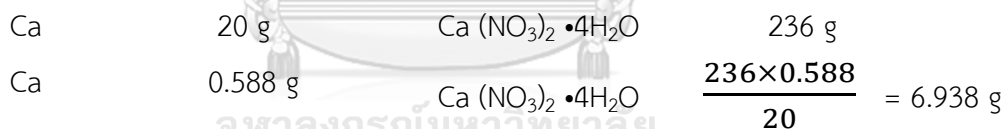
Second step,

Mw of Ca (NO<sub>3</sub>)<sub>2</sub> •6H<sub>2</sub>O = 272 g/mol

Mw of Ca = 20 g/mol



Third step, Fixed: Ca = 0.588 g ; Mw of Ca (NO<sub>3</sub>)<sub>2</sub> •4H<sub>2</sub>O = 236 g/mol



## Appendix C

### Yield efficiency calculation

The yield efficiency is defined in equation below

$$\text{yield efficiency} = \frac{\text{Amount of product produced (g)}}{\text{Power supplied } \left(\frac{\text{J}}{\text{s}}\right) \times \text{reaction time (s)}}$$

For example, calculated yield efficiency of RPB reactor.

Power of RPB reactor = 92.3 (W, J/s)

Power of peristaltic pump (oil+ methanol) =27.8 (W, J/s)

Power of heat oil =258.1 (W, J/s)

Power of water bath =205.6 (W, J/s)

Power of stirrer methanol =21 (W, J/s)

Total power = 604.8 W

Biodiesel yield = 98.68%

g of oil = 184.84 g at total flow rate 130 ml/min

At first step, the selection of 98.68% biodiesel yield was converted to g of actual methyl ester.

So, g of actual methyl ester is equal to  $\frac{184.84\text{g} \times 98.68\%}{100\%} = 182.40\text{ g}$

Second step, calculation of yield efficiency

$$\text{Yield efficiency} = \frac{182.40(\text{g})}{604.8 \left(\frac{\text{J}}{\text{s}}\right) \times 3.8 (\text{s})} = 40.9 \text{ g/J}$$

**VITA**

**NAME** Patcharaporn Sukjarern

**DATE OF BIRTH** 08 March 1995

**PLACE OF BIRTH** Nakornsrihammarat

**INSTITUTIONS ATTENDED** Department of Chemical Engineering, Faculty of Engineering, Rajamangala University of Technology Thanyaburi

